

# Synthesis and applications of anisotropic nanoparticles with precisely defined dimensions

Pearce, Amanda K.; Wilks, Thomas; Arno, Maria Chiara; O'Reilly, Rachel

DOI:

[10.1038/s41570-020-00232-7](https://doi.org/10.1038/s41570-020-00232-7)

License:

Other (please specify with Rights Statement)

*Document Version*

Peer reviewed version

*Citation for published version (Harvard):*

Pearce, AK, Wilks, T, Arno, MC & O'Reilly, R 2021, 'Synthesis and applications of anisotropic nanoparticles with precisely defined dimensions', *Nature Reviews Chemistry*, vol. 5, no. 1, pp. 21–45.  
<https://doi.org/10.1038/s41570-020-00232-7>

[Link to publication on Research at Birmingham portal](#)

## **Publisher Rights Statement:**

Subject to Springer Nature re-use terms: <https://www.nature.com/nature-research/editorial-policies/self-archiving-and-license-to-publish#AAMtermsV1>

## **General rights**

Unless a licence is specified above, all rights (including copyright and moral rights) in this document are retained by the authors and/or the copyright holders. The express permission of the copyright holder must be obtained for any use of this material other than for purposes permitted by law.

- Users may freely distribute the URL that is used to identify this publication.
- Users may download and/or print one copy of the publication from the University of Birmingham research portal for the purpose of private study or non-commercial research.
- User may use extracts from the document in line with the concept of 'fair dealing' under the Copyright, Designs and Patents Act 1988 (?)
- Users may not further distribute the material nor use it for the purposes of commercial gain.

Where a licence is displayed above, please note the terms and conditions of the licence govern your use of this document.

When citing, please reference the published version.

## **Take down policy**

While the University of Birmingham exercises care and attention in making items available there are rare occasions when an item has been uploaded in error or has been deemed to be commercially or otherwise sensitive.

If you believe that this is the case for this document, please contact [UBIRA@lists.bham.ac.uk](mailto:UBIRA@lists.bham.ac.uk) providing details and we will remove access to the work immediately and investigate.



# **Synthesis and applications of anisotropic nanoparticles with precisely defined dimensions**

*Amanda K. Pearce, Thomas R. Wilks, Maria C. Arno and Rachel K. O'Reilly<sup>†</sup>*

School of Chemistry, University of Birmingham, Edgbaston, Birmingham, B15 2TT, UK.

<sup>†</sup>Corresponding author: Rachel K. O'Reilly (r.oreilly@bham.ac.uk)



## **ABSTRACT**

Shape and size play a powerful role in determining the properties of a material, therefore controlling these aspects with precision is an important, fundamental goal of the chemical sciences. In particular, the introduction of shape anisotropy at the nanoscale has emerged as a potent way to access new properties and functionality, enabling the exploration of complex nanomaterials across a range of applications. Recent advances in DNA and protein nanotechnology, inorganic crystallisation techniques and precision polymer self-assembly are now enabling unprecedented control over the synthesis of anisotropic nanoparticles with a variety of shapes, encompassing one-dimensional rods, dumbbells and wires, two- and three-dimensional platelets, rings, polyhedra, stars and more. This has in turn enabled much progress to be made in our understanding of how anisotropy and particle dimensions can be tuned to produce materials with unique and highly optimised properties. In this Review, we bring these recent developments together to critically appraise the different methods for the bottom-up synthesis of anisotropic nanoparticles enabling exquisite control over morphology and dimensions. We highlight the unique properties of these materials in arenas as diverse as electron transport and biological processing, illustrating how they can be leveraged to produce devices and materials with otherwise inaccessible functionality. By making size and shape our focus, we aim to identify potential synergies between different disciplines and produce a roadmap for future research in this crucial area.

## **[H1] Introduction**

Anisotropy, the display of direction-dependent behaviour, is a fundamental property of our universe. It underpins the existence of complex systems, from the formation of solar systems to cell division. It is often said that for living systems equilibrium is death and the same could be applied to isotropy – an isotropic cell would be incapable of any of the complex behaviours necessary to sustain life. Indeed, the importance of anisotropy at the macro level is so obvious that it is easy to take it for granted. It seems intuitive that anisotropic building blocks will be required to create structures with any



kind of functional complexity. There is no reason this rule should not continue to hold at much smaller length scales, and nature provides us with a wealth of examples of the exploitation of anisotropy to create highly functional materials. Tubulin, the scaffolding of the cell, is assembled into a network of high-aspect-ratio nanorods that can be reconfigured on demand in response to environmental signals.<sup>1</sup> Bone derives its enviable combination of stiffness and toughness from the assembly of anisotropic components across multiple length scales.<sup>2</sup> The iridescence of bird and insect wings originates from the way in which light interacts with their asymmetric nanoscale features.<sup>3</sup>

Chemists have been attempting to emulate the structural and functional complexity found in nature for many years in an effort to access ever more complex materials for applications from energy harvesting to drug delivery. Anisotropy at the nanoscale in particular has been shown to enable significant advances in materials performance. For example, solar cells based on anisotropic nanostructures can achieve greater light harvesting efficiency than those made from simple, isotropic building blocks,<sup>4</sup> and the ability of worm-like nanoparticles to act as viscosity modifiers has been appreciated and exploited by industry for some time.<sup>5</sup> Anisotropic nanoparticles behave very differently in vivo from their isotropic counterparts, and it is increasingly being recognised that particle shape is a vital design parameter for realising the next generation of nanomedicines.<sup>6,7</sup>

The general effect of anisotropy on the properties of nanoscale systems is well appreciated. Therefore, a natural follow-up question is: how can anisotropy be controlled to tune material properties? If we again look to biology, we observe that precise control of anisotropy is required to unlock advanced functionality. One of the best-known examples is the packaging of RNA in tobacco mosaic virus capsids, which consists of precisely-defined nanorods constructed from 2130 copies of a capsomer protein.<sup>8,9</sup> However, the controlled construction of anisotropic nanoparticles is not trivial for a chemist. For example, it is relatively straightforward to produce worm-like nanoparticles through the self-assembly of synthetic polymers,<sup>10</sup> but controlling their aspect ratio is almost impos-



sible using conventional methods such as solution processing and polymerisation-induced self-assembly (PISA)..<sup>10,11</sup> These challenges have historically limited studies into the precise effects of shape and size on nanoparticle properties, ultimately restricting our understanding of how best to optimise nanoparticle design for different applications.

The past two decades have witnessed the rapid development of new methods that allow anisotropic nanoparticles to be prepared with a high degree of precision.<sup>12–16</sup> This has enabled researchers to begin probing nanoparticle structure–function relationships in unprecedented detail.<sup>17–22</sup> This Review describes these recent advances in our control and understanding of nanoparticle anisotropy, in an effort to promote cross-fertilisation of ideas between the diverse set of disciplines involved. Studies that make use of well-defined anisotropic nanostructures (that is, with a single morphology and with narrow size distributions) and the insights these give us into how tuning shape allows us to accurately control materials properties will be the particular focus. The discussion will generally be confined to particles with dimensions on the nanoscale (less than  $\sim 1\text{ }\mu\text{m}$ ) and to shape anisotropy, as opposed to chemical anisotropy (see Box 1), which has been extensively reviewed elsewhere.<sup>23–28</sup> Our aim is to present a roadmap for future directions in this vital emerging area of materials research.

## **[H1] Synthesis**

Making structurally anisotropic nanoparticles is not in itself challenging. For example, it has been known for some time that certain surfactants preferentially assemble into worm-like nanoparticles in water.<sup>29</sup> Similarly, amphiphilic block copolymers can be designed to assemble into anisotropic structures by controlling the balance between solvophobic and solvophilic segments.<sup>30</sup> Metal and other materials such as silica and carbon can be induced to grow into anisotropic shapes by careful control of processing conditions.<sup>31</sup> However, systematic control of the dimensions of the resulting nanoparticles using these methods is considerably more challenging as it requires precise control over the na-



noparticle formation process. If the synthesis of the nanoparticles is under thermodynamic control (for example, surfactant self-assembly), no single size is favoured because there is not a large difference in stability between particles with different aspect ratios.<sup>32</sup> If the particle formation relies on kinetic trapping of the product (for example, metal nanoparticle growth, polymerisation-induced self-assembly), the simultaneous control of the different processes involved in nanoparticle growth (such as, nucleation and elongation) becomes difficult. However, over the past thirty years these limitations have been circumvented, and several different approaches for the construction of anisotropic nanoparticles are available that enable excellent levels of dimensional control, which are reviewed in the following section. We have chosen to focus solely on bottom-up assembly methods because, compared to top-down approaches, they are more informative about fundamental self-assembly processes, have greater potential for the alteration of particle internal structure, and allow access to a wider range of aspect ratios and smaller particle sizes. Top-down methods have been covered extensively in recent reviews, to which the reader is referred.<sup>6,33–38</sup>

## **[H2] Controlled crystallisation**

The most established method for making anisotropic nanoparticles is that of the controlled crystallisation of molecular or atomic building blocks (Figure 1). A simple model for crystal growth is expressed by the LaMer phase diagram (Box 2), which separates the process into distinct nucleation and growth stages. According to this model, it is theoretically possible to grow precisely defined nanoparticles composed of any crystalline material starting from dissolved molecular precursors, as long as the appropriate conditions can be found. This method of mixing building blocks in solution and then exposing them to particular growth conditions for a set amount of time is often referred to as solvothermal synthesis (Figure 1, route 1). This has furnished a remarkable array of nanoparticles with controlled shapes and sizes from the nanometer to micron length scale, and made from a variety of materials (for example, metal oxides, silica, and metal-organic frameworks (MOFs)).<sup>39–48</sup> However, the yields of the desired nanoparticle morphology produced by solvothermal methods are high-



ly variable, ranging from almost quantitative to very low (less than 10%). One reason for this is that there is a technological limit to how precisely parameters such as purity, temperature and pH can be regulated: any slight variation from the desired conditions can result in loss of control. A second more fundamental reason is that it has become increasingly clear that in many, if not all, crystallisation processes several growth pathways are possible that operate alongside and compete with the classical route (Box 2).<sup>49</sup> Optimised conditions for one pathway may therefore lead to loss of control in another. Even when yields can be optimised, the most significant drawback of solvothermal synthesis from the point of view of controlling shape and dimensions remains: because of the almost infinite variety of additives and experimental parameters that can be tuned, it is practically impossible, for many systems, to predict a priori which conditions will give rise to which particle shape and size. For certain materials, however, advances in fundamental understanding have led to remarkable improvements in our ability to rationally tune reaction conditions to target particular morphologies. For example, a theoretical study of the growth mechanism of Au nanoparticles has offered insights on how to achieve the surfactant-free growth of a wide range of gold nanostructures. The pristine surface of these gold particles resulted in superior performance in applications such as catalysis compared to structures with surfaces passivated by structure-directing ligands.<sup>50</sup>

A powerful alternative approach to solvothermal synthesis is to separate the seed formation and growth phases, in what is usually called ‘seeded’ growth (Figure 1, route 2). Small, well-defined nanoparticles are first formed and purified, if necessary, then used as seeds in a second, separate growth step. This approach means that nucleation and growth conditions can be tuned independently. Seeded growth was first used for the synthesis of rod-shaped metal nanoparticles,<sup>31,44</sup> but the approach has now been demonstrated for a large variety of materials including metal oxides,<sup>43,51,52</sup> semiconductors,<sup>53,54</sup> metal-organic frameworks (MOFs),<sup>42,55</sup> silica,<sup>56</sup> graphene,<sup>57,58</sup> organic small molecules<sup>59,60</sup> and polymers.<sup>61</sup> It is a mature technology that allows access to a bewildering variety of shapes and sizes with excellent dimensional control. The main advantage of seeded growth over sol-



solvothermal synthesis is that control over nanoparticle size is made easier — larger particles can be grown simply by varying the duration of the growth step (Figure 1, step 2b). This means that it is relatively straightforward to produce particles that vary only in their dimensions in contrast to solvothermal methods in which different sizes are accessed by changing the concentrations of additives, the solvent and/or the pH, which can lead to changes in surface chemistry. Despite these advantages, for the majority of materials, finding the best conditions for the nucleation and growth steps still involves a large amount of trial and-error, which is often time-consuming and leads to concerns about reproducibility.

Recent advances in seeded growth have addressed, to some extent, some of the above shortcomings. A good example is the development of crystallisation-driven self-assembly (CDSA, Figure 2a). CDSA makes use of block copolymers containing one or more solvophilic blocks attached to a semi-crystalline block. When placed in a poor solvent for the semi-crystalline block and heated above the glass transition temperature, crystallisation is induced, leading to nanoparticles stabilised by a corona of the solvophilic block. This initial crystallisation affords nanoparticles of different sizes, which can be fragmented, for example by sonication, into small, well-defined seed nanoparticles and used in a controlled growth step to achieve dimensional precision. Although most reports of CDSA separate the seed synthesis and growth steps, one-pot methods have recently been reported, simplifying the process.<sup>62–65</sup> The key advantage of CDSA over the seeded growth of small molecule building blocks is that the polymer components can be readily tuned to influence the outcome of the growth process. For example, a rod- or plate-shaped morphology can be selected simply by tuning block ratios (Figure 2b).<sup>66</sup> Similarly, the depths of platelets and the diameters of rods can be altered by simple changes to the lengths of the polymer segments. The surface and corona chemistries can be altered by using different solvophilic polymers and by modifying the polymer end groups.<sup>67</sup> This flexibility has made it possible to grow nanoparticles with complex topologies (Figure 2c) and multifunctional structures with well-defined domains of different polymers (Figure 2d), which begins to



approach the kind of hierarchical control over self-assembly seen in biology.<sup>68–72</sup> CDSA therefore represents an attractive platform for seeded growth because of the extent to which the growth process can be rationally tuned by simple alterations to the polymer components. However, the search for suitable seed formation and growth conditions remains largely empirical and greatly varies not only between different materials but also within the same polymer, when different solvophobic to solvophilic ratios are used.

Ideally, it would be possible to completely rationally design a system that would crystallise into a pre-determined shape with precisely controlled nanoscale dimensions. One way of achieving this is to take inspiration from polymer science. The development of controlled polymerisation techniques has enabled the synthesis of macromolecules with controlled lengths. This is achieved through a variety of mechanisms, but all have in common an initiation step followed by chain elongation. Key to control is that monomers only react with the active chain end and not with each other. Extension of this principle to the assembly of small molecule building blocks into nanoparticles could provide a route to the fully rational engineering of shape and size. Towards this end, several groups have recently reported controlled supramolecular chain growth polymerisation.<sup>59,60,73</sup> A supramolecular cyclic ‘monomer’ has been designed that exists as a dormant species owing to the formation of intramolecular hydrogen bonds (H-bonds).<sup>60</sup> Polymerisation is initiated by a modified monomer with the intramolecular H-bonds removed, which activates the next added monomer, allowing it to attack another monomer, and so on. Control over the length of rod-like nanoparticles was demonstrated using this approach, as well as the ability to distinguish between different enantiomers of the monomer, which is an excellent illustration of the kind of atomic level precision accessible through these systems. Although this approach has largely been limited to the production of one-dimensional rod-like structures, research is progressing to the synthesis of 2D and 3D structures by design of appropriate building blocks.<sup>74</sup>



## [H2] Programmed assembly

Seeded growth is a kinetically controlled process. An alternative approach is to rely on thermodynamics to drive what may be thought of as the ‘programmed assembly’ of nanoparticles (Figure 3a). In this case, one or more macromolecules fold into a specific shape, driven by specific inter and intramolecular interactions. This approach is routinely used by nature in the folding of proteins into the fabulous array of complex 3D shapes found in biological systems. Perhaps the simplest particles obtained using this approach are single chain nanoparticles (SCNPs).<sup>75–79</sup> Several anisotropic shapes are accessible by programmed assembly of SCNPs, including worms,<sup>80</sup> tadpoles,<sup>81,82</sup> dumbbells<sup>83</sup> and complex multicyclic systems<sup>84,85</sup>, but most are small (<10 nm) because even very long linear polymers do not take up much volume when collapsed (for example, hydrodynamic radius of a 86 kDa poly(ethylene glycol) chain is only 9.5 nm).<sup>86</sup> This limitation can, however, be overcome by making polymers with very long, bulky side-chains, usually referred to as ‘bottlebrush’ polymers. The bottlebrush polymer structure can be tuned to force it to adopt anisotropic worm-like or other more unusual morphologies (Figure 3b, left).<sup>87,88</sup> Nevertheless, a limitation of these polymers is that they lack perfectly defined sequences, which is highly likely to limit their ability to reliably fold into more complex structures,<sup>76</sup> for which a sequence-defined macromolecule is thought to be required. An excellent example is DNA, which can be synthesised with perfect sequence control using solid phase chemistry or enzymatically. DNA base pairing is highly stable and predictable, making this material ideal for the precise construction of nanoscale objects. This concept was first realised several decades ago by Seeman,<sup>89</sup> but became more widespread following the invention of the DNA origami approach by Rothemund (Figure 3b, middle).<sup>90</sup> The unique appeal of DNA nanotechnology is that it gives access to anisotropic shapes of far greater complexity and with higher precision than accessible through controlled crystallisation processes. Advances in the design and synthesis of DNA nanostructures mean that it is now possible to create complex 3D shapes of almost arbitrary design.<sup>91–93</sup> The introduction of functionalised DNA allows these structures to be further elaborated



for specific applications. However, DNA is an extremely costly material to work with, which hinders its large-scale application. Although this limitation may be overcome in the future by employing biotechnological mass production methods,<sup>94</sup> a further issue is that modifying the chemical composition of DNA nanostructures is possible only to a limited extent. Ultimately, the final structure will be made of DNA, which may lead to undesirable properties for particular applications. For example, DNA nanostructures bear a high degree of negative charge, which can impede cell uptake.<sup>95</sup>

Compared with DNA, proteins offer much more flexibility in terms of chemical composition, because they are composed of a broader range of building blocks (21 naturally occurring amino acids versus 4 nucleobases). However, while DNA folds very predictably following a simple set of rules, protein folding is orders of magnitude more complex because of the numerous weak and, in some cases poorly understood, molecular interactions involved, leaving the design of protein assemblies from scratch as an unmet goal. Nevertheless, this has not stopped huge progress being made in the controlled assembly of engineered proteins. By starting from sequences that are already known to reliably fold into particular structures, it has been possible to focus efforts on tuning these structures to control their higher order assembly.<sup>96</sup> One approach has been to tune the curvature of protein interfaces to furnish anisotropic nanostructures, as has been demonstrated in the production of a range of complex structures.<sup>97</sup> For example, nanorings of different diameters have been assembled from protein subunits.<sup>98</sup> To further increase the geometrical complexity available to protein nanostructures, engineering efforts have focused on methods to build polyhedra<sup>99, 100</sup>. Related work has also seen the engineering of precisely-defined barrel-shaped nanostructures by rational design of coiled peptides (Figure 3b, right)<sup>101, 102</sup>. However, these structures so far remain small (<20 nm) compared with their DNA origami cousins, which can now reach several hundreds of nanometres in size.<sup>103</sup> On a simpler level, it is possible to re-purpose native proteins to form anisotropic structures, as was applied for the construction of nanotubes with defined lengths by using bacteriophage protein components, for example.<sup>104</sup> Although there are numerous examples of the supramolecular polymerisation



of protein subunits into larger anisotropic assemblies, to date the vast majority of these studies have not focused on exerting control over all particle dimensions, usually focusing on tuning a single parameter such as diameter. Combining advances in protein engineering and supramolecular polymerisation could enable protein nanostructures to reach larger length scales. This could have a dramatic impact on our ability to create precision anisotropic nanostructures with a high degree of functionality, with further potential for very fine control over chemical reactivity.

## **[H2] Templated assembly**

Controlled crystal growth and programmed assembly can only be performed with certain materials. The use of other building blocks is, however, possible through templated assembly (Figure 4). In this case, well defined nanoparticles, made by one of the approaches described above, are used to direct the assembly of a second material. The following discussion describes three approaches to templated assembly.

One way to perform template assembly is by ‘coating’, which is the deposition of other materials on the surface of a nanoparticle (Figure 4a). A very simple example is deposition of a second metal layer on a gold nanorod.<sup>105</sup> In biology, coating is thought to be exploited by certain viruses, which can self-mineralise to preserve their integrity in extreme environments.<sup>106</sup> Some viral capsids are themselves the product of a templated assembly — the tobacco mosaic virus (TMV) capsid’s length, for example, is controlled by the length of the RNA sequence it contains.<sup>107</sup> With the exception of an initiation domain, the RNA sequence can be elongated or truncated to produce viral nanoparticles with highly controlled lengths.<sup>108</sup> These viral nanoparticles can then be further coated with a large variety of materials, furnishing well-defined anisotropic nanoparticles with varied compositions.<sup>109–</sup>  
<sup>112</sup>More recently, DNA origami nanostructures have been mineralised, giving access to exquisitely well-defined silica or calcium phosphate-coated nanostructures.<sup>113–115</sup> This complements the rich literature around the metallation of DNA nanostructures, which is by now a well-developed field.<sup>116–118</sup>



DNA origami scaffolds have also been demonstrated to direct the assembly of lipids into structures that are not normally accessible, such as cuboids.<sup>119</sup> A benefit of the coating approach that should be noted is that the template can sometimes actively encourage materials that are challenging to crystallise on their own to form ordered structures. For example, crystallisation of a normally challenging MOF has been achieved by using a more stable MOF as an underlying template.<sup>120</sup>

Another approach to templated assembly is ‘casting’, wherein a hollow anisotropic nanoparticle is used as a mould (Figure 4b). This approach is less common than coating, most likely because suitable hollow nanoparticles are more difficult to access. However, tubular viral capsids have been extensively explored to cast nanowires and nanoparticle chains.<sup>121</sup> DNA nanostructures have also been used with this approach, for example gold nanostructures of various shapes have been grown within the cavities of DNA origami moulds.<sup>122–125</sup> A recent development has been the use of DNA moulds to direct the assembly of softer materials, such as lipid membranes.<sup>126</sup> For example, modulation of membrane shape using reconfigurable DNA nanostructures has been demonstrated, with control over curvature and width, but not length.<sup>127</sup> The interior of a DNA nanotube was also used to template the polymerisation of dopamine.<sup>128</sup>

The final and most sophisticated form of templated assembly is the ‘breadboard’ approach (Figure 4c). A nanoscale pattern is used to direct the assembly of building blocks with much greater precision than is possible with coating or casting. For example, engineering of viral coat proteins gives capsids with functional groups displayed at particular locations, and these can be used to direct the placement of other materials.<sup>106</sup> DNA origami structures can be used in a similar way. In a recent example, controlled placement of thiol groups on a DNA origami triangle was exploited to direct the growth of a variety of metal and metal oxide shapes that would be very difficult to grow through crystal growth techniques.<sup>129</sup> A follow-up study described the successful growth of silica nanostruc-



tures using the same approach, further broadening the scope.<sup>130</sup> DNA was also used to controllably place mineralising groups to achieve controlled growth of calcium phosphate.<sup>131</sup>

One of the great potential advantages of the breadboard approach is the possibility for re-use of the template, something that is difficult to achieve with coating and casting. A proof of concept illustration of this approach was recently reported by Sleiman and co-workers.<sup>132</sup> In their ‘assemble, grow and lift-off’ (AGLO) strategy, DNA-coated gold nanoparticles are positioned in a desired pattern by hybridisation to complementary DNA strands displayed on a DNA origami tile. Controlled decomposition of gold salts then fuses the particles, fixing them permanently into the desired shape. A variety of shapes were made using this method, but more importantly the template was re-used for a second round of AGLO. A similar approach was used by Weil and co-workers to template the polymerisation of dopamine<sup>133</sup> and methacrylates,<sup>134</sup> illustrating the potential flexibility of this approach to be applied to other materials. The process requires further optimisation to improve the yield of the desired shape, and improve recovery of the template, but it has huge promise for the creation of mixed material nanoparticles with highly controlled shapes and sizes.

## **[H1] Properties and Applications of Anisotropic Nanoparticles**

The methods discussed above would have remained scientific curiosities were it not for the fact that the shape and size of a nanoparticle have been shown to have a substantial, sometimes drastic, influence on its properties and therefore subsequent applications. Anisotropy, in particular, leads to a whole host of physical, chemical and biological effects inaccessible to isotropic systems, as has been reviewed in several recent contributions.<sup>6,7,135</sup> However, the majority of studies in this area have focused on comparing isotropic particles with a single (often disperse) sample of anisotropic particles.<sup>6,10,44,45,135</sup> Investigations into the differences between nanoparticles of different shapes (isotropic and anisotropic) and dimensions but the same surface chemistry are extremely rare. These kinds of studies may lead to a much more detailed understanding of how a nanoparticle’s parameters



are related to its properties and how they can be further exploited to achieve application end goals. Below, we summarise what has been reported to date, specifically focusing on properties and applications of anisotropic nanoparticles which have been synthesised through synthetic methods that allow for precise control over their dimensions and discussed in the previous section. Furthermore, we focus on identifying emerging opportunities and challenges.

## **[H2] Optical and electronic properties**

The precise effects of nanoparticle dimensions on light–matter interactions have been studied in detail, at least for metal and inorganic particles.<sup>31,136</sup> Particle anisotropy introduces additional surface plasmon resonance (SPR) modes, and the positions of the resulting absorption bands can be tuned by modifying the dimensions and shape of the particle. Early examples demonstrated how tuning the aspect ratio of gold nanorods resulted in a shift in the longitudinal SPR band into the infrared.<sup>137,138</sup>

The position and intensity of the SPR peaks in anisotropic metal nanostructures are also much more sensitive to perturbations in the local environment (such as the binding of ligands, or changes in solvent polarity) than the isotropic equivalents<sup>139</sup>, which is the reason for their popularity in sensing applications.<sup>140–142</sup> In a pivotal example, Orrit and co-workers<sup>143</sup> demonstrated how the precise control of the length of gold nanorods led to their applications in single-molecule detection based on SPR. They described a 37 nm gold nanorod end-functionalized with biotin to which the single-molecule binding could be detected by monitoring longitudinal SPR with photothermal microscopy. The magnitude of the photothermal signal could be maximised by tuning the length of the nanorod, and thus matching the surface plasma absorption spectra with the heating laser wavelength (785 nm), highlighting the importance of precise control over nanoparticle dimensions. Similarly, the variable of the width of gold nanorods was also studied to further increase the signal-to-noise ratio<sup>144</sup>. The nanorod diameter was modulated in the range between 10 and 50 nm and a S/N >1 was found for



particle widths between 20 and 45 nm (aspect ratio 2.25). These insights not only contribute to improved single-molecule detection, but may also progress the use of such sensors in other applications including plasmon rulers, hydrogen sensors and in the biomedical field.

El-Sayed and co-workers<sup>145</sup> were the first to exploit gold nanorods for combined imaging and therapy, selectively targeting malignant tumour cells over healthy cells (Figure 5). Increasing the aspect ratio of the nanoparticles over a range of 2.4 to 5.5 caused a tuneable shift of their surface plasmon absorption spectra further into the NIR region, giving improved in vivo tissue penetration over their spherical counterparts (from less than 500  $\mu\text{m}$  to approximately 10 cm), greatly increasing the treatment scope. The selected nanorods with aspect ratio 3.9 achieved specific binding to malignant cells over normal cells, resulting in a distinctive diagnostic scattering image compared to normal cells. Importantly, this specificity also reduced the laser power needed to cause destruction of the malignant cells to avoid death to non-malignant cells, and overall achieving a lower absorption threshold energy than had previously been reported for other NIR absorbing nanoparticles. It is of significance that this dual performance selectivity was possible only because of a precise control over nanoparticle anisotropy.

Perhaps more interestingly, the absorption spectra of gold and silver nanoparticles have been shown to depend intimately on their shape (Figure 6a), giving researchers the ability to further modulate these properties through access to branched nanostars, nanoplates, nanocubes and a variety of polyhedrons.<sup>146–150</sup> Such anisotropic shapes also exhibit high electric fields at their extremities, for example, at the tips of nanorods or the sharp edges of nanostars in the so-called ‘lightning rod’ effect<sup>151</sup>. This effect, coupled with their strong absorption in the NIR, make anisotropic nanoparticles excellent materials for surface-enhanced Raman scattering (SERS), the sensitivity of which has been shown to be substantially affected by shape and size of the nanoparticles (Figure 6b).<sup>152</sup> The local electromagnetic field strength and redshift of the SPR can be increased by forming ‘hotspots’ resulting from



surface roughness, interactions between a particle and metal surface or aggregations between multiple particles, or it can be increased through manipulating the local curvature of the metallic nanoparticles. This effect was investigated by directly comparing SPR and SERS of gold nanospheres, their aggregates, nanotriangles and nanostars using a model probe molecule (rhodamine 6G, R6G).<sup>21</sup> As expected, a negligible SERS was observed for gold nanospheres of 150 nm, although their aggregates ( $\sim 1\ \mu\text{m}$ ) exhibited a slight redshift, whereas the SPR maxima and resultant SERS response were further increased for the 135 nm nanotriangles and particularly 148 nm nanostars. Although one can easily control the number of local field hotspots for different nanoparticle shapes, controlling the effect of surface chemistries on these properties is more difficult.

On account of their high concentration of local field hotspots and thus strong SERS response, the potential of selective cancer imaging agents based on gold nanostars has been further explored using nanoparticles comprising of a 75 nm star-shaped gold core and a silica shell (overall diameter 140 nm)<sup>153</sup>. The shell featured a Raman reporter molecule in resonance with the NIR laser at 785 nm, yielding surface-enhanced resonance Raman scattering (SERRS) nanostars. Currently, the inability to visualize the true extent of cancers represents a significant challenge in many areas of oncology. Tumour detection is often limited to sites of high nanoparticle uptake owing to the low SERS signal strength, meaning that precancerous lesions or micrometastases remain undetected. In vivo the SERRS nanostars could not only detect macroscopic tumours, but also microscopic and premalignant lesions with sensitivity nearly 400 times higher than the nonresonant counterparts<sup>153</sup>. In this clinical context, SERS is promising as a highly sensitive and precise imaging modality because of the molecular Raman fingerprints and resonance in the NIR window.

Other than therapeutic and diagnostic applications, the effect of shape modulation was also investigated on properties such as the photoluminescence in lead halide perovskite nanoribbons<sup>154</sup> (Figure 6c) and CdSe quantum dots.<sup>54</sup> A high density perovskite nanowire array was used to elegant-



ly create a biomimetic electrochemistry artificial eye<sup>155</sup>. The hemispherical nanowire photosensors were comprised of formamidinium lead iodide (FAPbI<sub>3</sub>) and acted as the retina, sandwiched between an ionic liquid electrolyte as the vitreous humour and liquid-metal wires to mimic human nerve fibres behind the retina. The imaging resolution, response and recovery times and spectral responsivity were comparable with human photoreceptors in the retina and cone cells., Overall, this biomimetic eye achieved high-resolution image-sensing ability as demonstrated by the reconstruction of projected optical patterns using recording and conversion of the resultant photocurrent.<sup>155</sup>

The electron transport properties of anisotropic nanoparticles have also been studied in detail for several decades.<sup>156</sup> As the size of a crystal approaches the nanometre regime, its size and shape begin to influence its behaviour because quantised (rather than continuous) states begin to emerge.<sup>157</sup> As a result, the importance of controlling the sizes and shapes of nanostructured domains has become increasingly apparent in fields such as light harvesting,<sup>158</sup> energy storage<sup>159</sup> and photonics.<sup>160,161</sup> In particular, 1D nanostructures including nanowires have been used to increase the efficiencies of devices such as solar cells and lasers.<sup>160,162</sup> It has become clear that the dimensions of the structures are important in optimising device performance, but current production methods (usually top-down) can make it challenging to tune dimension along specific directions, which has led to contradictory results. For example, it has been reported that nanowire length influences transport properties, with longer wires giving more efficient devices,<sup>163,164</sup> but these studies have been confounded by the fact that nanowire diameter tends to increase along with length.<sup>165</sup> A more recent investigation in which diameter, length and nanowire spacing were carefully controlled showed that transport properties are length-independent, which underscores the importance of achieving better control in these systems.<sup>166</sup> The benefits of better structural control in this context was also illustrated by using CDSA to make a series of well-defined ribbon-like nanoparticles of length between 180–1900 nm containing complementary semiconducting polymers (polythiophene and poly(di-*n*-hexylfluorene))<sup>167</sup>. By controlling the spatial separation of the components and optimising the di-



mensions of the structures, exciton transport was achieved over unprecedented length scales (>200 nm, Figure 7). This example highlights the potential for precision polymer-based nanostructures to match and extend the functionality of inorganic nanoparticles in optoelectronic applications, analogous to the rising use of organic materials in photovoltaic panels and LEDs.

## **[H2] Catalytic and magnetic properties**

Similarly with light and electronic properties, it has long been reported that metallic nanoparticles have catalytic activity and selectivity heavily influenced by their shapes and size. Uncontrolled production of nanoparticles of different shapes results in different kinds of active species, which exhibit different reactivities and usually lower activity and selectivity overall. Higher fractions of surface atoms have been observed on sharp corners and edges of metallic nanocatalysts. Therefore, a precise control over particle dimensions and shape, as well as crystallographic facets, ultimately determine the number of active surface sites. Early studies demonstrated lower activation energies and average rate constants for tetrahedral platinum nanocrystals over cubic or spherical morphologies,<sup>168</sup> higher catalytic activity for polygonal gold nanoparticles compared to spherical ones<sup>169</sup> and higher specific reaction rates for 50 nm silver nanocubes with {100} planes than for 50 nm spherical nanoparticles and 200 nm nanoplates with {111} planes (Figure 8a),<sup>170</sup> although these nanoparticles were produced through synthesis techniques that did not allow for precise control over their dimensions. Platinum multiarm nanostars synthesised through a seed-mediated method demonstrated higher activity, although the number of arms within each particle could not be controlled.<sup>171</sup> Similar results were observed for highly faceted multioctahedral nanocrystals<sup>172</sup> and branched nanoparticles.<sup>173</sup> Huang and co-workers produced a range of gold nanoparticles using AgNO<sub>3</sub>-assisted synthesis obtaining shape-, size- and length-controlled decahedra (ranging from 21 to 81 nm), bipyramids (144 nm and 150 nm) and rods (ranging from 85 to 126 nm in length) through manipulation of reaction conditions.<sup>174</sup> The resultant particles exhibited size- and structure-dependent catalytic performance in the reduction of *p*-nitrophenol to *p*-aminophenol by sodium borohydride. Single-crystal dendritic



platinum nanoparticles of 20 nm (distance point-to-point) have also been synthesized and were assembled onto the surface of carbon nanotubes, yielding a homogeneously loaded hybrid catalyst with clean Pt surfaces<sup>175</sup>. The multiple corners and edges of the dendritic particles are more active for the reduction of hexacyanoferrate(III) by sodium borohydride compared with spherical nanoparticles.

In general, the properties of magnetic materials are determined by both their electronic and crystal structures, therefore anisotropic nanoparticles can give rise to interesting properties owing to an interplay between magnetocrystalline anisotropy, shape anisotropy and crystal surface facets.<sup>176</sup> While spherical nanoparticles can be magnetised homogeneously, elongated particles such as nanorods, nanotubes and nanowires are more easily magnetised along the long axis and plate-like particles perpendicular to the basal plane, and therefore can produce an anisotropic response to magnetic fields.<sup>45</sup> However, it remains a challenge to synthesise non-spherical magnetic nanoparticles through traditional seeded growth mechanisms because of the inherent isotropic crystal structure of magnetic materials.<sup>177,178</sup> Therefore the majority of the anisotropic magnetic nanoparticles are produced through templated or top-down methods, or through routes that do not allow for size and/or shape control.<sup>45</sup> Of most interest here is solvothermal synthesis using shaping ligands.<sup>179</sup> Length-controlled FePt nanorods and nanowires (of length between 20 nm and 200 nm) were grown within surfactant cylindrical micelles and could be assembled into anisotropic magnetically aligned nanomagnet arrays.<sup>180,181</sup> A similar approach was used to produce monodisperse 10 nm × 7 nm Mn<sub>3</sub>O<sub>4</sub> nanoplates with ferromagnetic behaviour.<sup>182</sup> The importance of shape anisotropy is highlighted by the comparison of superparamagnetic spherical cobalt nanoparticles versus monodisperse and monocrystalline ferromagnetic cobalt nanorods and nanowires at room temperature. Furthermore, the latter could self-organise into 2D and 3D superstructures with potential application in magnetic data storage.<sup>183,184</sup> Co<sub>3</sub>O<sub>4</sub> octahedra with tuneable sizes of 20, 40 and 85 nm (edge length) were ferromagnetic owing to a combination of the specific displayed nanocrystal morphology of {111} surface facets and their small lateral



size. Thus, shape and size control were crucial for obtaining an overall ferromagnetic behaviour in otherwise antiferromagnetic particles.<sup>176</sup>

In the bulk state platinum is nonmagnetic, but becomes magnetic at the nanoscale level and particularly so for anisotropic particles.<sup>185</sup> When branched platinum nanocrystals were synthesised using annealing temperature and reaction time to control size and morphology producing 8 nm elongated nanoparticles and 9 nm tetrapods, enhanced ferromagnetism (10 times larger) was observed compared with 8 nm spherical nanoparticles at room temperature.<sup>186</sup> Magnetisation was further enhanced by a factor of 8 for dodecanethiol-capped platinum branched tetrapods compared with oleylamine-capped particles, suggesting an additional contribution of charge transfer from the coating surfactant that causes a localised permanent magnetic moment. The ability to control morphology of platinum nanocrystals to synthesise Pt–ZnO composite nanoparticles with interesting catalytic and magnetic properties was also demonstrated.<sup>187</sup> The investigation of different morphologies of the seed crystal and platinum nanocrystals with different exposed facets revealed that the truncated octahedral morphology had enclosed {111} and {100} facets, which allowed for selective growth of zinc from the {111} facets. The use of the truncated octahedral seeds led to composite ZnO–Pt nanoflowers with enhanced photocatalytic activity owing to exposed Pt{100} facets as reaction sites and electron transfer from ZnO to Pt. Furthermore, the unique morphology provided enhanced ferromagnetism compared to the pure materials.

The well-reported plasmon-resonance of gold nanostars was further exploited to produce dynamic gyromagnetic imaging contrast agents through the introduction of a 13 nm Fe<sub>3</sub>O<sub>4</sub> superparamagnetic core in gold nanostars.<sup>188</sup> The multiarmed gold nanostars had an average size of 100 nm and, despite their structure not being perfectly homogenous, this study elegantly demonstrated a polarisation-sensitive scattering of the magnetically responsive particles to a rotating magnetic field gradient for bioimaging applications. The anisotropic nature of the gold shell was crucial to achieve



polarisation-dependent scattering at NIR frequencies, leading to gyromagnetic contrast as a consequence of the synchronisation of the magnetic moment with the polarised emission. The resultant particles were explored for their ability to be selectively imaged following receptor-mediated uptake into tumour cells and exposure to a polarised NIR laser beam ( $\lambda_{\text{ex}}=780$  nm) for selective excitation of the nanostars. The resultant scattering was visualized under both conventional (time-domain) and gyromagnetic imaging conditions, whereby Fourier transform of the gyromagnetic signals had enhanced signal-to-noise and signal-to-background ratios inside tumour cells compared with the time-domain imaging. The Fourier-domain imaging also produced clear resolution, thus demonstrating a route to overcome low signal intensities in time-domain imaging.

A particular advantage of anisotropic magnetic structures is the ability to selectively align the particles in response to an applied magnetic field.<sup>189–191</sup> Gold nanorods were attached to  $\text{Fe}_3\text{O}_4$  nanorods, so that the orientation of the former relative to incident light, and thus their plasmonic excitation modes, could be magnetically controlled.<sup>189</sup> These structures exhibited a highly sensitive colour switching behaviour in response to the changing orientation and strength of the applied magnetic field by emitting alternative green and red light under illumination and while self-rotating under a magnetic stirring field. Similarly, ferromagnetic ellipsoidal  $\text{FeSiO}_2$  colloidal photonic structures of 190 and 220 nm in length were prepared and could spontaneously order into colloidal crystals (Figure 8b).<sup>191</sup> It was possible to tune the reflection wavelength of these particles by changing the magnetic field direction with respect to the incident light. The nanorods could also be dispersed within a UV curable resin producing thin film liquid crystals, where patterns of different polarisation and control over transmittance of light could be achieved through the magnetic field responsivity.<sup>190</sup> These examples open new strategies towards building active optical components, creation of photonic patterns under magnetic fields, and selective chemical and biomedical sensors.



## [H2] Fluid behaviour

The dispersion of nanoparticles in fluids has become an extremely important area of research. ‘Nanofluids’ have a number of desirable properties compared to simple liquids including enhanced heat transfer and friction reduction, making them perfectly suited to industrial applications that require efficient lubrication and cooling.<sup>192,193</sup> Anisotropic nanoparticles behave very differently under flow compared to their isotropic analogues,<sup>5</sup> opening the door to further enhancement of nanofluid properties. When exposed to high shear rates, liquids containing anisotropic nanoparticles exhibit shear-thinning and other non-Newtonian behaviours,<sup>194</sup> which makes them extremely useful for a number of applications ranging from industrial lubrication to polymer processing. In addition, the enhanced thermal transport properties exhibited by many anisotropic nanoparticles means they can be employed as very effective coolants.<sup>195</sup> However, the rheological behaviour of anisotropic particles is highly complex and not captured fully by current models.<sup>192–194</sup> A full understanding of their rheological behaviour therefore requires a combination of theory, molecular modelling and experimental work. Developments in the theoretical understanding of these systems have suggested a rich interplay between the effects of shape and other properties such as charge,<sup>18,196</sup> enabling complex and potentially useful behaviours to be realised. However, examples of empirical studies in which the dimensions of nanoparticles are systematically varied are rare, possibly because this field has traditionally made use of particles such as clay nanosheets, for which well-controlled syntheses have yet to be developed.<sup>197</sup> Furthermore, when particle size has been controlled, there often exist confounding factors that make it difficult to draw clear conclusions about the effect of aspect ratio on flow behaviour. For example, the rheological properties of carbon nanofibers of different lengths between 5 to 100  $\mu\text{m}$  have been studied, but because these fibres were obtained using two different processing routes, it was not possible to conclude whether geometry or changes in surface chemistry were the cause of the observed differences in their physical behaviour.<sup>198</sup> The study of the rheological properties of 2D nanoplates made of mineral kaolinite revealed very similar behaviour for plates



with two different aspect ratios.<sup>199</sup> On the contrary, different aspect ratios of zirconium phosphate platelets led to marked differences in the properties imparted to epoxy resins.<sup>200</sup> White and co-workers have investigated the precise effects of aspect ratio on the rheology of 2D platelet nanoparticles and observed notable deviations from theory for particular shapes – for example, large aspect ratio particles showed unusual shear thinning and thickening behaviours. The study also emphasised the role that less considered factors, such as rigidity, may play in determining rheological properties.<sup>201</sup>

Although our fundamental understanding of how particle anisotropy can influence fluid behaviours remains limited, anisotropic nanoparticles are increasingly used as viscosity modifiers in a range of applications such as engine lubricants.<sup>202</sup> This has naturally led to investigations on the impact of structure on performance, for example, worm-like or cylindrical micelles are of interest owing to their ability to align in flow. However, resistance to shear thinning has a dependence on cylinder length and chain entanglement, but also varying the cylinder thickness can change the time of disentanglement, with implications in resistance to high shear<sup>203</sup>. Molecular properties such as micelle thickness were observed to influence shear rate and shear viscosity. Thicker surfactant-based micelles had shorter breaking times that resulted in the onset of shear thinning at higher shear rates. Conversely, block copolymer cylinder micelles with narrower dimensions (ranging from 6 nm to 13 nm) exhibited shear thinning and cylinder orientation at lower shear rates. This means that the efficacy of cylindrical particles to modulate fluid properties such as for thickeners, drag reducers and flow improvers can be tuned through control over nanoparticle dimensions.

## **[H2] Gelation and interfacial interactions**

Access to non-spherical morphologies, particularly worms, has enabled the formation of soft, free-standing gels in aqueous solution simply by exploiting inter-particle entanglement.<sup>71,204,205</sup> Although anisotropic nanoparticles have been widely used to induce gelation and increase the mechanical



properties of hydrogels, the use of non-spherical nanostructures of controlled size for this purpose has been limited.<sup>206,207</sup> For example, fibre-reinforced colloidal hydrogels have been synthesised for applications in regenerative medicine. By controlling the aminolysis process of polydisperse poly-*L*-lactic acid (PLLA) fibers, rod-shaped particles with tuneable size were obtained and incorporated into intercolloidal hydrogel networks fabricated using spherical gelatin nanoparticles as colloidal building blocks.<sup>208</sup> Shorter fibres were shown to distribute better throughout the gels and interact stronger with gelatin nanoparticles as a result of their higher specific surface area.

Cellulose nanocrystals (CNCs) — bio-based rigid rod-shaped particles derived from cellulose— have been widely used to reinforce hydrogel networks. Commonly, CNCs are prepared by sulfuric acid hydrolysis of cotton or wood pulp, which imparts anionic sulfate half ester groups on the nanoparticle surface.<sup>209,210</sup> CNCs have been incorporated in non-injectable hydrogels through physical entrapment or chemical crosslinking to increase the hydrogel's mechanical properties<sup>211–214</sup> and introduce anisotropy<sup>215,216</sup> or macroporosity.<sup>217–219</sup> While CNCs form a gel at a concentration of 10 wt%, CNC as additive fillers are incorporated into pre-formed hydrogels at low concentration, inducing modification into hydrogel properties without disrupting the 3D network.<sup>220</sup> Notably, few reports have demonstrated the use of CNCs as mechanics-enhancing agents in injectable hydrogels.<sup>221</sup> This has been observed in sequentially covalent–ionic cross-linked alginate–gelatin hydrogels, whereby alginate and gelatin were pre-cross-linked using carbodiimide chemistry, mixed with a suspension of CNCs to form an injectable hydrogel precursor, and then mixed with  $\text{Zn}^{2+}$  ions to form a stronger network.<sup>222</sup> Physical entrapment of CNCs within the gel led to a 1.8-fold increase in compressive modulus (up to 92 kPa) versus gels prepared without any CNCs. Other ionically cross-linked hydrogels composed of cationic quaternized cellulose and anionic  $\beta$ -glycerophosphate with physical incorporation of cationic CNCs, led to a two-order increase of the energy storage modulus relative to the CNC-free gel owing to enhanced charge screening and hydrogen bonding.<sup>223</sup>



Polymerisation-induced self-assembly (PISA) can also lead to in situ gel formation.<sup>224</sup> Such gels exhibited unique properties, including thermoresponsive and reversible gelation as a result of temperature induced worm-to-sphere transitions. However, this work was based on anisotropic structures with poorly defined lengths. Tuning nanoparticle dimensions may therefore provide another level of control over hydrogel properties. This has recently been demonstrated using CDSA, either by epitaxial growth directly in water<sup>71</sup> (Figure 9a) or by enriching the polymeric hydrogel matrix with pre-formed nanoparticles of different shapes and sizes.<sup>225</sup> Dove, O'Reilly and colleagues reported the first example of controlled CDSA in water using poly(caprolactone), a degradable, crystalline polymer.<sup>71</sup> The sizes of the resulting 1D nanoparticles could be tailored to a desired uniform length directly in water. A steady increase in solution viscosity was observed until a critical length was reached (2  $\mu\text{m}$  in this case), when physical entanglement of the cylinders led to hydrogel formation, generating an injectable strong material that could be used for cell encapsulation.

In a second example, the mechanical properties of translationally relevant alginate hydrogels were tuned by incorporating separately prepared 0D, 1D and 2D PLLA-based nanoparticles in the biopolymer matrix.<sup>225</sup> The greater surface area per particle offered by the 2D platelets led to more, and, therefore, stronger interactions with the alginate, enhancing the gel's mechanical properties compared to spherical (0D) and cylindrical (1D) particles. A suspension of platelets was also used as a glue between alginate hydrogel blocks and bovine cartilage strips, showing superior adhesive properties compared to spherical and cylindrical micelles.

1D and 2D nanoparticles of controlled dimensions have been used to stabilize water-in-water and water-in-oil Pickering emulsions, which are formed when two incompatible polymers are mixed above certain threshold concentrations<sup>226–228</sup> and play an important role in different areas, including green chemistry,<sup>229,230</sup> cell biology<sup>226</sup> and food industry.<sup>231</sup> Although clay nanosheets,<sup>232,233</sup> Janus nanoparticles,<sup>234</sup> which surface is characterised by two or more distinct physical properties, and inor-



ganic lamellar crystals<sup>235</sup> have been used to stabilise Pickering emulsions, all of these have been produced using top-down self-assembly approaches. Herein, we will only consider particles that are synthesized using a bottom-up methodology. Non-spherical particles leads to solid–liquid interface-mediated capillary forces.<sup>236–238</sup> Young’s equation requires that at the three-phase contact line the angle between the interface and the colloid surface is equal to the solid–liquid contact angle  $\theta$ . For spatially anisotropic surfaces, this condition cannot be met when the interface remains flat, hence capillary attractive interactions are induced.<sup>238,239</sup> Using a series of haematite particles of the same surface chemistry and size (synthesised by forced hydrolysis of  $\text{Fe}^{\text{III}}$  in the presence of urea), it was demonstrated that stable emulsions can be obtained using a particle concentration from 1 to 10%.<sup>240</sup> As a consequence of the increased effective surface coverage and the occurrence of shape-induced capillary forces, strong but brittle elastic surface gels could be obtained. Furthermore, the control over the emulsion stability was closely linked to the particle aspect ratio and surface coverage.

Theoretical investigations of the effect of aspect ratio on the strength of adhesive interactions between anisotropic particles and solid surfaces revealed significant differences in the energy barrier to adhesion.<sup>241</sup> Long, thin cylinders were found to have a much lower energy barrier to attachment than shorter, wider ones. Substantial differences have also been observed between hollow and solid particles, with implications across diverse fields including bacterial adhesion. Although these findings have yet to be tested experimentally, there has been a promising report on the ability of 2D CDSA platelets to stabilise liquid–liquid interactions in a Pickering emulsion, with larger platelets giving smaller, more stable droplets (Figure 9b).<sup>242</sup>

Ultrathin, gibbsite colloidal platelets have been observed to stabilise water-in-water emulsions.<sup>243</sup> Small platelets (170 nm in length) were found to cover the droplet surface in a more uniform fashion than larger platelets, hence stabilising the emulsion more effectively. Large platelets (700 nm in length) not only rendered the droplets heavy, but also settle at the bottom of each droplet,



leaving it less stabilised at the top and hence leading to a lower stabilisation of the emulsion. Overall, compared to nanospheres, nanoplatelets are better suited to stabilise Pickering emulsions, as a consequence of their ability to block a relatively large area of the water–water interface without causing the droplets to become heavy and sediment. Rod-shaped cellulose nanocrystals with an anisotropic parallelepiped structure (160 nm × 6 nm × 6 nm) have also been used as water-in-water emulsion stabilisers in a dextran–poly(ethylene oxide) (PEO) emulsion.<sup>244</sup> As a consequence of the high anisotropy of the rod like materials, less material is needed to stabilise water-in-water emulsions than when homogeneous spherical colloids are used. Cellulosic colloidal nanorods of different origins were also used to investigate the effect of various elongated shapes adsorbed at the oil–water interface.<sup>245</sup> Nanocrystals of length ranging from 185 nm to 4 µm were obtained from the hydrolysis of cellulose microfibrils of three different origins: cotton, bacterial cellulose and *Cladophora*, leading to aspect ratios ranging from 13 to 160. The three different types of nanocrystals were irreversibly adsorbed at the oil–water interface and form stable emulsions.

## **[H2] Biological interactions and therapeutics**

For more than thirty years, nanotechnology has promised to deliver a new generation of more effective, safer medicines by enabling their targeted delivery to the site of disease. It is increasingly appreciated that in order to realise this promise we must move beyond simple isotropic nanoparticle designs.<sup>6,7</sup> Anisotropic morphologies enable more directed and specific interactions with biological systems at the molecular, cellular and tissue levels,<sup>6,246–248</sup> however the exploitation of nanoparticle anisotropy in the drug delivery field has vast untapped potential. Until recently, the difficulties in precisely controlling nanoparticle dimensions and shapes for polymeric materials through bottom-up self-assembly methods have limited investigations to rigid inorganic particles and/or top-down synthesis approaches, thus leaving the field overall in its infancy. Over the last decade researchers have shifted focus to study the cellular internalisation behaviour of non-spherical morphologies, inspired by the varied shapes of virus particles.<sup>249</sup> Early work in this field by Chan and co-workers began to



shed light on the influence that nanoparticle size could have in mediating biological effects, for example targeted nanoparticle toxicity through modulation of cellular pathways as a result of specific nanoparticle size.<sup>250,251</sup> Beyond this, shape has also been shown to influence biological behaviours such as circulation lifetimes, extravasation through tissues and distribution in vivo.<sup>252</sup> Cylindrical micelles and rods demonstrate persistent blood circulation times of up to one week post-injection and decreased interactions with macrophages. However, cellular uptake can be dependent on aspect ratio owing to cylinder alignment in flow, therefore it is essential to maintain complete control over nanoparticle dimensions.<sup>20,247,253,254</sup> These biological properties give particular promise for applications in blood diseases such as leukemia, where there is no fixed disease site and the ideal therapy can reach the entire circulatory system with a long residence time. In this regard, superparamagnetic anisotropic drug-loaded iron oxide nanoparticles using a static magnetic field-assisted assembly approach have been synthesized (Figure 10b)<sup>255</sup>. Compared with isotropic particles, cylindrical assemblies could maintain a higher concentration of the loaded drug within the blood for a longer time period, as well as decreased clearance rates of the particles from the body. They also observed that the anisotropic particles displayed a preference to remain in the circulation and had less liver and spleen sequestration compared to the isotropic particles. This promoted a greater therapeutic effect, which was reflected by decreased leukocyte counts and CD13 expression (a cell-surface protease aminopeptidase that positively influences tumour growth) after 1 week of administration. Potentially, disc-shaped hydrophilic nanoparticles can achieve even better circulation kinetics, specificity and efficiency of cellular uptake compared with rods and spheres.<sup>256–259</sup> The advent of new methodologies for precisely controlling particle dimensions has enabled researchers to explore in even greater depth the biological properties of anisotropic nanoparticles, particularly for soft, organic materials, widening the scope of work possible in this area.

The dimensions of a polymer particle have implications on cellular uptake behaviour and controlled bottom-up synthetic methods, as described above, provide the ideal tool for reliably probing



this phenomenon. Previous work has shown direct comparison between spherical and rod-like particles, however often these studies are limited to only a few aspect ratios, giving little indication of the exact tunability of cellular uptake response with particle shape. For example, DNA-nanoparticles of highly controlled rod morphology have been found to significantly enhance cell internalization compared to spherical nanoparticles<sup>260</sup>. The same effect was observed in vivo for quantum dot-based spheres and rods, the latter being more amenable to transport and distribution into tumours<sup>254</sup>. An interesting study of anisotropic structures in the context of finding more efficient therapeutic strategies arose from the hypothesis that the size and dynamics of single membrane transporters could be investigated using gold nanorods and *Pseudomonas aeruginosa* as a model living cell<sup>261</sup>. The implications of increased understanding in the way cells interact with biomaterials and extrusion mechanisms of both particles and drugs are important to avoid multidrug resistance. By modulating the length of gold nanorods (52 nm, 74 nm and 97 nm) it was possible to image directly the dynamics of membrane permeability. This led to the observation that interactions between membrane proteins and particles could trigger formation and assembly of additional membrane transporters for extrusion of substrates. The uptake and efflux dynamics of the nanoparticles were heterogeneous across individual bacteria, providing important insights at a single-membrane-pump level into mechanisms of resistance, with potential impact downstream in drug delivery particle design.

To date, advanced applications of anisotropic nanoparticles have overwhelmingly been dominated by noble metal nanoparticles as a consequence of the more developed precision syntheses of these materials. It would be of great interest to study these advantages in the biological fields in further depth using a wider range of materials and morphologies, such as 2D platelet structures. CDSA has proved to be particularly useful in this regard. The assembly process can generate morphologies from spheres to rods to platelets while maintaining the same surface chemistry.<sup>67,262–267</sup> Exploiting this methodology, Li and co-workers<sup>268,269</sup> were able to fabricate polymeric nanocylinders and different shape of nanoplatelets directly in water, all featuring a polysaccharide corona for investiga-



tions into particle shape-dependent interactions with macrophages. They observed that cylinders had far higher cellular uptake than any platelet particles. However, when the activation of macrophages was investigated, platelets showed stronger stimulated secretion of pro-inflammatory cytokines, despite the lower rate of endocytosis (Figure 10a). This was also related to the size of platelet particles, with smaller platelets having the greatest macrophage stimulation efficiency, highlighting the impact of highly controlled nanoparticle anisotropy in potential immunotherapy applications. This strategy was further demonstrated by Inam and co-workers<sup>270</sup> who explored the antibacterial activity of 2D polymer assemblies through CDSA. In this case, small platelets exhibited higher antibacterial activity than large platelets or spherical structures, providing a useful tool for exploring how antibacterial activity of nanoparticles can be controlled through morphology and size effects.

In the bloodstream, the shapes of white blood cells and platelets have evolved to enable long circulation times, and to increase the frequency of interactions with the blood vessel walls to facilitate the search for vascular abnormalities.<sup>258</sup> Mimicking this kind of behaviour could lead to improved efficacy for nanoparticle therapeutics, for example by enabling them to move more easily through vascular fenestrations or bind with disease-specific vascular receptors. Indeed, disc or platelet shaped nanoparticles have been revealed to have unique *in vivo* behaviours, such as greater organ accumulation with less liver sequestration compared to spherical or cylindrical particles.<sup>271</sup> In a further study, it was shown that medium-sized platelet particles ( $1000 \times 400$  nm plateloids) demonstrated the best hydrodynamic forces and interfacial interactions required for efficient tumour accumulation even without the use of specific targeting ligands, with small platelets ( $600 \times 200$  nm) accumulating more extensively in the liver and spleen, and large platelets ( $1800 \times 600$  nm) in the lungs (Figure 10c)<sup>272</sup>. Other factors that are important for nanoparticle distribution *in vivo* have received limited attention in terms of the effects of size and shape. For example, the effect of aspect ratio on the types of proteins accumulated by two different gold nanorods ( $40 \times 11$  and  $70 \times 15$  nm) and stars ( $40$  and  $70$  nm external diameter).<sup>273</sup> Significant differences in the total amount of protein and the types



and variety of proteins adsorbed on the nanoparticle surface were observed, but the study was limited to nanoparticles made of a single material (gold) and by the availability of different aspect ratios and shapes.

Overall, it is clear that nanoparticle shape strongly dictates biological properties such as circulation lifetimes, cellular internalisation and interactions with proteins, with clear preference thus far for cylindrical nanostructures in this regard. However, predominately studies probing these fundamental nanoparticle interactions have used inorganic-based materials. Moving forward it will be of interest to extend this work into soft matter particles, such as through CDSA, as controlled synthesis techniques continue to develop.

## **[H1] Outlook**

This Review has illustrated the sheer breadth of areas in which precision anisotropic nanoparticles could have, or in some cases are already having, a transformative impact. However, there remain a number of challenges to overcome before the full potential of these materials can be realized. In this final section we highlight what we believe to be the most important areas for future work, in an effort to lay out a roadmap for those working in the field (Figure 11).

## **[H2] New synthetic methods**

As detailed above, there are now numerous methods available for the precise bottom-up assembly of anisotropic nanoparticles. Although these methods encompass a very broad range of different approaches, a single challenge unites them: expanding the range of materials that can be used as building blocks. The following section expands on how we postulate this might be achieved in each of the three general synthetic approaches we have identified.

Controlled crystallisation techniques have enabled important advances in our ability to make precision anisotropic nanoparticles. However, it remains challenging to rationally control nanoparticle shape and size through modulation of reaction conditions. CDSA provides one route around this is-



sue, but other approaches are needed. Advances in our understanding of crystallisation processes will be vital,<sup>274</sup> but bringing the power of evolution to bear on the synthesis of anisotropic nanoparticles can also be advantageous. Microbes and other organisms use specific proteins to exert precise control over the growth of mineral nanoparticles, such as the diverse array of anisotropic magnetite ( $\text{Fe}_3\text{O}_4$ ) nanoparticles grown inside many bacteria.<sup>275,276</sup> Staniland and co-workers have demonstrated how these protein motifs can be taken out of their biological context to control mineralisation in vitro.<sup>277</sup> Beyond this, ‘bio-panning’ allows the in vitro evolution of peptides<sup>278,279</sup> and nucleic acids<sup>280–286</sup> that control the growth of an increasingly large array of materials. Use of evolution greatly accelerates the discovery of ligands capable of controlling nanoparticle synthesis, a process that has traditionally relied on serendipity and trial-and-error.

A more fundamental limitation of controlled crystallisation is that it requires the use of materials that form well-ordered domains. Although there have been recent reports using more unusual interactions as the basis for seeded growth, such as hydrogen bonding,<sup>198</sup>  $\pi$ – $\pi$  interactions<sup>287</sup> and metal–metal bonding<sup>288</sup>, we believe a priority for the field should be the identification of growth mechanisms that enable the controlled growth of nanostructures based on amorphous materials. A recently proposed approach, based on a morphological transformation process (MORPH) exploits supramolecular bonding to drive insertion of a polymer into a spherical seed nanoparticle, coupled with careful design of the polymers’ physical properties, to control growth of amorphous, high aspect ratio wormlike nanoparticles<sup>289</sup>. A physical model developed to describe this ‘morphological transformation’ process suggested that it should be possible to use other supramolecular bonding interactions to achieve similar results. If this proves to be the case, then it will represent a useful complementary technique to seeded growth for the production of precisely defined anisotropic nanoparticles.

Another synthetic challenge is to expand the scope of the thermodynamic self-assembly of anisotropic nanostructures. Protein engineering is already producing complex shapes, but these are lim-



ited in size; achieving control over protein oligomerisation could be one way to overcome these limitations. A modular systems of protein ‘rods’ and ‘connectors’ has been proposed that enables the programmable assembly of complex nanoscale shapes based on engineering of gamma-prefoldin, a protein from a deep sea thermophilic bacterium whose native function is to assist in the folding of other proteins.<sup>290</sup> Taking further inspiration from the hierarchical assembly of DNA origami structures may also be a promising avenue: simple design rules can be used to control the hierarchical assembly of DNA tiles, giving access to structures at the micron scale while retaining structural precision.<sup>291</sup> Alternatively, taking a biohybrid approach may be fruitful, as illustrated by the growing field of DNA–protein origami.<sup>292</sup> In this approach, engineered proteins are used as highly controllable, modular linkers to join rigid DNA helices together in a designed pattern.

Ultimately, the goal must be to move beyond biomolecules for programmed assembly. The development of peptide nucleic acid (PNA), in which the DNA phosphate backbone is replaced with peptide linkages, is a simple step in this direction.<sup>293</sup> Taylor and co-workers recently reported the first successful formation of complex PNA nanostructures in organic solvents, an environment inaccessible to DNA, and we believe this kind of approach has a promising future in the context of anisotropic nanoparticles.<sup>294</sup> Replacing the natural bases with artificial groups goes one step further into the emerging area of the synthesis and programmed self-assembly of sequence-defined polymers.<sup>295</sup> The self-assembly of poly(phosphoesters) has been reported to be determined by monomer sequence, a vital first step in achieving the level of controlled folding possible with biomolecules.<sup>296</sup> Given the success of the DNA origami approach in this context, it is worth asking what features a synthetic analogue would need to mimic in order to be useful. Building nanostructures from DNA has become incredibly popular because of three very attractive features: the development of computational design tools (such as caDNAno<sup>297</sup>) that allow users to draw a desired shape and have the required DNA sequences automatically generated; the availability of synthetic DNA made by solid phase synthesis; and the simplicity of the experimental protocols for folding DNA nanostructures. The solid phase



synthesis of different sequence-defined polymers is a rapidly advancing field,<sup>298–301</sup> but less attention has so far been paid to controlled molecular folding and we expect this to be an exciting emerging field in the years to come. The advances in folding of SCNPs described in this Review give just a hint of what will become possible in the near future.

Even with the advances discussed so far, for many materials the direct formation of well-defined anisotropic nanostructures will remain out of reach. We believe that templated assembly has great untapped potential to address this problem. The redirection of viral coat protein assembly using non-natural nanostructure templates is a rapidly developing field, with recent examples using branched RNA,<sup>302,303</sup> DNA,<sup>304,305</sup> polymers,<sup>306</sup> metal nanorods<sup>307</sup> and supramolecular amphiphile structures.<sup>308</sup> This idea was recently extended to the assembly of viral coat protein mimics.<sup>309,310</sup> Going further, plasmid DNA was used to direct the self-assembly of synthetic polymers, with different shapes accessible depending on the conformation of the plasmid (itself controlled by changes in ionic strength).<sup>311</sup> Another report used intercalation to drive the association of polymers with double stranded DNA, and demonstrated that rod-like nanoparticles with defined dimensions could be generated, with their lengths determined by that of the templating DNA helix.<sup>312</sup> Extending this general approach to more complex templates (for example branched and topologically complex shapes) and more diverse materials will yield interesting results. On a more simplistic level, advances in the controlled deposition and growth of secondary materials on precision structures made through CDSA of block copolymers or DNA origami would enable many interesting new studies. The recent reports on mineralisation of DNA nanostructures provide some hint of the future possibilities and the exquisite control that can be obtained.<sup>313</sup> Furthermore, bottlebrush SCNPs can be used as highly controllable templates for the growth of anisotropic nanostructures,<sup>314</sup> building on previous work from Muller and coworkers.<sup>315</sup> This approach is highly versatile as the template can be readily tuned by simply altering the length and composition of the polymer using controlled polymerisation techniques.<sup>88</sup>



We believe the methods with the greatest potential are the casting and breadboard approaches, because they make recycling of the template possible. This is important because template costs are presently high (as in the case of those based on biomolecules) – reuse means that a single template can produce many copies of the product, reducing the overall cost. Hollow 3D structures are yet to be made by CDSA. However, when they are achieved they will be ideal moulds for casting other materials because they can be more robust than DNA origami, which is usually unstable to the presence of large amounts of organic solvent and/or low salt concentrations. There is a growing interest in controlled polymerisation within viral cages<sup>316</sup>. Although current examples are limited to isotropic structures, expanding this to anisotropic capsids such as that of TMV could represent a useful new approach to casting polymer nanostructures. Further development of the breadboard approach to allow easier reuse of the template and a wider array of materials is also an exciting area to watch. An interesting example was recently published by Belcher and coworkers, who used a DNA origami tile as a template to cut carbon nanotubes to precise lengths determined by the width of the tile.<sup>317</sup>

## **[H2] Understanding properties**

Our understanding of the properties of anisotropic nanoparticles is currently rather incomplete. A great deal of fundamental work has been done in the area of light–matter interactions and electron transport, enabling rational design of nanoparticle dimensions for particular applications. In almost every other area where anisotropic nanoparticles have been shown to exhibit unique properties, meanwhile, our understanding of how to control these properties remains lacking. As described above, to date anisotropic nanoparticles have been explored across a vast area of application, including optical and electronics, catalysis and magnetism, gelation and interfacial interactions, fluid behaviour and a range of biological interactions and therapeutics. However, it is apparent that the slow development of synthetic methods to access particle anisotropy is a significant bottleneck in the process towards a full understanding of possible achievable properties. The advantage of an anisotropic particle over an isotropic one has been demonstrated for certain applications, but often only for a



single type of material or a limited variety of shapes. This limits our understanding of how many properties can be introduced through particle shape and what other factors should be considered, such as the presence of crystallinity or particular chemistries. This can be exemplified in the area of thermal properties of anisotropic conducting materials, in which thus far investigations have been limited by the availability of controlled synthesis routes towards these materials, and as such is an exciting field with unknown potential.

Given the rapid recent developments in dimensional control of soft matter materials, we believe it would be of great interest to compare and contrast areas previously explored with materials such as transition metals, and we believe that CDSA is the most logical approach for this purpose, purely as a result of the extensive studies and literature reports thus far. While some fields such as catalysis and magnetism can only be explored for limited classes of materials, for other areas such as light harvesting, energy storage and photonics, we see opportunities for the precision nanoparticles accessible through CDSA. These obtained particles can be used in model systems to determine how device efficiency can be optimised. The recent functionalization of a range of different surfaces using CDSA [\[Au: Edit OK?\]](#) will open up exciting new opportunities in this area, by making it possible to straightforwardly modify different substrates with nanoparticles of precise shape and size in a single step.<sup>318</sup>

We believe there is huge potential for the translation of precision nanoparticles made using CDSA into the realm of rheology modification. As discussed above, the rheology of anisotropic nanostructures presents numerous challenges to theorists and modellers alike. However, the precisely-defined cylindrical and platelet structures accessible through CDSA, the surface compositions of which can also be tuned to a high degree, make these nanoparticles ideal model systems for studying how such parameters affect industrially important properties including shear thinning and thickening behaviour, thermal transport, lubrication and wear reduction.



Perhaps the area in which precision nanoparticles have the greatest unrealised potential is therapeutics. It is now widely accepted that nanoparticle shape plays a vital role in mediating how these materials are recognised, processed and excreted by the body. The surprising wealth of literature to date would suggest that anisotropic shapes, particularly elongated rods or worms, hold the greatest potential for next generation therapeutic constructs.<sup>20,253,319–321</sup> This is based on the observed enhanced cell uptake that results from the increased ligand interactions and other improved biological behaviours such as circulation lifetimes, extravasation through tissues and distribution in vivo in comparison to spheres. However, given the previous difficulties in precisely controlling nanoparticle dimensions using traditional polymer self-assembly techniques, not to mention the ability to independently control shape, surface chemistry and composition, only a small number of studies can truly examine the effects of aspect ratio on biological processing, which has in turn hindered our ability to draw unambiguous conclusions thus far. It is important to also consider the less widely explored influence of nanoparticle rigidity on these properties. For example, it is highly possible that a flexible cylindrical particle will demonstrate enhanced cell uptake in comparison with a crystalline rod of similar dimensions, despite maintaining the same surface chemistry. As stated above, thus far such studies in this field have traditionally been performed on quite hard materials like silica or noble metal nanoparticles.<sup>17,250,322</sup> Moving forward, there is great scope and potential for investigations using the 1D and 2D polymer assemblies accessible through other bottom-up synthesis approaches. To realise a step change in the rate of progress in this area it will further be necessary to develop simple, rapid methods for the construction of nanoparticle libraries in which shape, size and chemical composition are independently varied. We believe controlled growth processes such as CDSA and MORPH have significant potential in this area.

## **[H2] Advanced applications**

We anticipate that the use of precision anisotropic nanoparticles to elucidate fundamental materials properties will naturally lead to their integration in advanced devices for a whole host of applica-



tions. One area with great potential is the integration of nanoparticles grown through CDSA of block copolymers into optoelectronic devices. The broader structural and chemical heterogeneity accessible to polymer-based systems in comparison to transition metals could mean much greater potential for tuning the properties of the resulting materials and, therefore, greatly improved device efficiency. Further development of CDSA to accommodate the use of more diverse polymers will be necessary, along with methods for the efficient integration of the products into functioning devices. The possibility for tuning shape, composition and surface chemistry could also be very interesting for making the next generation of nanofluids, in which precision anisotropic nanoparticles act as viscosity modifiers, adhesives, fillers and interfacial stabilisers with bespoke properties.

Nonetheless, it is our opinion that one of the most exciting fields to be opening as a result of the progression of nanoparticle dimensional control is within the biological realm. Crucial understandings of how nanomedicines interact with the body at the cellular and tissue levels will undoubtedly lead to full realisation of successful nanomedicines, diagnostics and tissue engineering. While CDSA appears to offer broad potential owing to easy access of anisotropic shapes and compatibility with biodegradable core-forming blocks such as poly(lactic acid) (PLA) and poly(caprolactone) (PCL), it is becoming apparent that less-developed processes involving templated and programmed assembly also warrant focus. Particularly templated assembly techniques such as the ‘breadboard’ approach can facilitate a high degree of versatility in chemical composition, as well as template recycling which increases feasibility. In addition, further developments in programmed assembly, such as folding of sequence-defined polymers and other biomimetic constructs like proteins and viruses, should provide great scope for reaching soft matter materials with absolute control over function and application. Undoubtedly the ability to precisely dictate nanoparticle dimensions while using a wide range of monomer building blocks can offer unprecedented influence over drug release rates, tissue accumulations, cellular processing and ultimately the efficacy that can be achieved. Anisotropic nanoparticles are already showing advantages for modifying essential hydrogel mechanical, viscoelas-



tic and adhesion properties, leading to materials with greater suitability for their intended application, for example scaffolds matching elastic modulus of tissues for greater cell regeneration.<sup>225</sup> The possibility to not only control nanoparticle shape to achieve these properties, but to also tailor the chemistry involved, can further introduce motifs for cell signalling or introduce active molecules with pre-determined release rates. The area of diagnostics will also benefit from an increased understanding of how nanoparticle shape can be more finely controlled with regards to noble metal materials. There is a rich history of SPR and SERS modulation with aspect ratio and shape, and a variety of resultant applications are beginning to be realized. Further developments in controlled synthesis of complex shapes such as nanostars and nanocages will surely lead to rapid progression in this area, as well as in related fields such as catalysis. Finally, there are scattered reports of anisotropic magnetic nano- or microparticles from uncontrolled synthetic strategies with interesting applications such as cell sensing and separation and probing cell rheology.<sup>323–325</sup> It would be of great interest to see where this field could progress as methods for production of magnetic particles with dimensional control continue to develop.

It is important to bear in mind that successful translation of a technology into ‘real world’ applications depends on a host of factors, not least among which is production cost. When considering the applications of the highly engineered nanoparticles discussed in this Review, it is therefore reasonable to raise concerns about whether the improved materials properties they enable will be enough to offset their high synthesis costs. A priority for those working in this field should be finding ways to bring these costs down and make synthetic routes amenable to scale-up that preserve reproducibility of particle shape and size. The recent development of polymerisation-induced CDSA is an excellent example of a move in this direction.<sup>318</sup> Drawing on inspiration from nature, which makes use of tightly controlled construction processes alongside error correction, may also be fruitful. However, even if industrial scale-up proves very difficult, precision anisotropic nanoparticles will still have a key role to play in realising next generation nanotechnologies. By serving as tools



that allow fundamental questions about nanoparticle structure–function relationships to be studied for the first time in a systematic manner, they will provide the empirical and theoretical rules we need to rationally design advanced materials using cheaper, more sustainable materials. It is this role as an ‘enabling’ tool that we think will be most important in the near future. Nowhere will this be more acutely appreciated than in nanomedicine, which for more than thirty years has failed to deliver on its great promise to revolutionise the way that disease is diagnosed and treated. With the unprecedented insights that precision nanostructures will give into the workings of the nano–bio interface, rationally designed nanoparticle therapies that overcome the current roadblocks associated with poor efficacy may finally be possible, and one of the long-held promises of nanotechnology realised at last.

#### **[H1] Acknowledgements**

**[Au: Please add here any acknowledgement if you wish to do so.]**

#### **[H1] Author contributions**

All authors contributed equally to the preparation of this manuscript. **[Au:OK?]**

#### **[H1] Competing interests statement**

**[Au: please declare any if you have them, including companies you are associated with]**

#### **[H1] ToC blurb**

The introduction of shape anisotropy at the nanoscale is a potent way to access new properties and functionality. This Review appraises different methods for the bottom-up synthesis of anisotropic nanoparticles, and highlights the unique properties and applications of these materials with otherwise inaccessible functionality.



[Au: Please write a 40-word summary of the article]

## References

1. Roostalu, J. & Surrey, T. Microtubule nucleation: beyond the template. *Nat. Rev. Mol. Cell Biol.* **18**, 702–710 (2017).
2. Reznikov, N., Bilton, M., Lari, L., Stevens, M. M. & Kröger, R. Fractal-like hierarchical organization of bone begins at the nanoscale. *Science (80-. ).* **360**, eaao2189 (2018).
3. Srinivasarao, M. Nano-Optics in the Biological World: Beetles, Butterflies, Birds, and Moths. *Chem. Rev.* **99**, 1935–1961 (1999).
4. Garnett, E. C., Brongersma, M. L., Cui, Y. & McGehee, M. D. Nanowire Solar Cells. *Annu. Rev. Mater. Res.* **41**, 269–295 (2011).
5. Litchfield, D. W. & Baird, D. G. The rheology of high aspect ratio nanoparticle filled liquids. *Rheol. Rev.* 1–60 (2006).
6. Meyer, R. A. & Green, J. J. Shaping the future of nanomedicine: Anisotropy in polymeric nanoparticle design. *Wiley Interdiscip Rev Nanomed Nanobiotechnol* **8**, 191–207 (2016).
7. Williams, D. S., Pijpers, I. A. B., Ridolfo, R. & van Hest, J. C. M. Controlling the morphology of copolymeric vectors for next generation nanomedicine. *J. Control. Release* **259**, 29–39 (2017).
8. Klug, A. The tobacco mosaic virus particle: structure and assembly. *Philos. Trans. R. Soc. B* **354**, 531–535 (1999).
9. Namba, K. & Stubbs, G. Structure of Tobacco Mosaic Virus at 3.6 Å Resolution: Implications for Assembly. *Science (80-. ).* **231**, 1401–1406 (1986).
10. Warren, N. J. & Armes, S. P. Polymerization-Induced Self-Assembly of Block Copolymer Nano-objects via RAFT Aqueous Dispersion Polymerization. *J. Am. Chem. Soc.* **136**, 10174–10185 (2014).
11. Mai, Y. & Eisenberg, A. Self-assembly of block copolymers. *Chem. Soc. Rev.* **41**, 5969–5985 (2012).



12. Huang, P. S. *et al.* High thermodynamic stability of parametrically designed helical bundles. *Science* (80-. ). **346**, 481–485 (2014).
13. Shenton, W., Douglas, T., Young, M., Stubbs, G. & Mann, S. Inorganic-organic nanotube composites from template mineralization of tobacco mosaic virus. *Adv. Mater.* **11**, 253–256 (1999).
14. Rothemund, P. W. K. Folding DNA to create nanoscale shapes and patterns. *Nature* **440**, 297–302 (2006).
15. Jana, N. R., Gearheart, L. & Murphy, C. J. Wet chemical synthesis of high aspect ratio cylindrical gold nanorods. *J. Phys. Chem. B* **105**, 4065–4067 (2001).
16. Wang, X. *et al.* Cylindrical block copolymer micelles and co-micelles of controlled length and architecture. *Science* (80-. ). **317**, 644–647 (2007).
17. Albanese, A., Tang, P. S. & Chan, W. C. W. The Effect of Nanoparticle Size, Shape, and Surface Chemistry on Biological Systems. *Annu. Rev. Biomed. Eng.* **14**, 1–16 (2012).
18. Heine, D. R., Petersen, M. K. & Grest, G. S. Effect of particle shape and charge on bulk rheology of nanoparticle suspensions. *J. Chem. Phys.* **132**, 184509 (2010).
19. Hinde, E. *et al.* Pair correlation microscopy reveals the role of nanoparticle shape in intracellular transport and site of drug release. *Nat. Nanotechnol.* **12**, 81–89 (2017).
20. Smith, B. R. *et al.* Shape matters: Intravital microscopy reveals surprising geometrical dependence for nanoparticles in tumor models of extravasation. *Nano Lett.* **12**, 3369–3377 (2012).
21. Tian, F., Bonnier, F., Casey, A., Shanahan, A. E. & Byrne, H. J. Surface enhanced Raman scattering with gold nanoparticles: Effect of particle shape. *Anal. Methods* **6**, 9116–9123 (2014).
22. Gerigk, M. *et al.* Nanoparticle shape anisotropy and photoluminescence properties: Europium containing ZnO as a Model Case. *Nanoscale* **7**, 16969–16982 (2015).
23. Ravaine, S. & Duguet, E. Synthesis and assembly of patchy particles: Recent progress and



- future prospects. *Curr. Opin. Colloid Interface Sci.* **30**, 45–53 (2017).
24. Pawar, A. B. & Kretzschmar, I. Fabrication, Assembly, and Application of Patchy Particles. *Macromol. Rapid Commun.* **31**, 150–168 (2010).
  25. Du, J. & O'Reilly, R. K. Anisotropic particles with patchy, multicompartment and Janus architectures: preparation and application. *Chem. Soc. Rev.* **40**, 2402–2416 (2011).
  26. Hu, J., Zhou, S., Sun, Y., Fang, X. & Wu, L. Fabrication, properties and applications of Janus particles. *Chem. Soc. Rev.* **41**, 4356–4378 (2012).
  27. Walther, A. & Müller, A. H. E. Janus particles: Synthesis, self-assembly, physical properties, and applications. *Chem. Rev.* **113**, 5194–5261 (2013).
  28. Zhang, J., Grzybowski, B. A. & Granick, S. Janus Particle Synthesis, Assembly, and Application. *Langmuir* **33**, 6964–6977 (2017).
  29. Israelachvili, J. N., Mitchell, D. J. & Ninham, B. W. Theory of self-assembly of hydrocarbon amphiphiles into micelles and bilayers. *J. Chem. Soc. Faraday Trans. 2 Mol. Chem. Phys.* **72**, 1525–1568 (1976).
  30. Mai, Y. & Eisenberg, A. Self-assembly of block copolymers. *Chem. Soc. Rev.* **41**, 5969–5985 (2012).
  31. Murphy, C. J. *et al.* Anisotropic metal nanoparticles: Synthesis, assembly, and optical applications. *J. Phys. Chem. B* **109**, 13857–13870 (2005).
  32. Israelachvili, J. N. Soft and Biological Structures. in *Intermolecular and Surface Forces* 535–576 (Academic Press, 2011). doi:10.1016/B978-0-12-375182-9.10020-X
  33. Merkel, T. J. *et al.* Scalable, Shape-Specific, Top-Down Fabrication Methods for the Synthesis of Engineered Colloidal Particles. *Langmuir* **26**, 13086–13096 (2010).
  34. Tang, Z. & Wei, A. Fabrication of anisotropic metal nanostructures using innovations in template-assisted lithography. *ACS Nano* **6**, 998–1003 (2012).
  35. Yu, H. D., Regulacio, M. D., Ye, E. & Han, M. Y. Chemical routes to top-down nanofabrication. *Chem. Soc. Rev.* **42**, 6006–6018 (2013).



36. Thorkelsson, K., Bai, P. & Xu, T. Self-assembly and applications of anisotropic nanomaterials: A review. *Nano Today* **10**, 48–66 (2015).
37. Xu, J. *et al.* Future of the particle replication in nonwetting templates (PRINT) technology. *Angew. Chemie - Int. Ed.* **52**, 6580–6589 (2013).
38. Fu, X. *et al.* Top-down fabrication of shape-controlled, monodisperse nanoparticles for biomedical applications. *Adv. Drug Deliv. Rev.* **132**, 169–187 (2018).
39. Cushing, B. L., Kolesnichenko, V. L. & O'Connor, C. J. Recent advances in the liquid-phase syntheses of inorganic nanoparticles. *Chem. Rev.* **104**, 3893–3946 (2004).
40. Wang, D. & Li, Y. Bimetallic nanocrystals: Liquid-phase synthesis and catalytic applications. *Adv. Mater.* **23**, 1044–1060 (2011).
41. Jun, Y. W., Choi, J. S. & Cheon, J. Shape control of semiconductor and metal oxide nanocrystals through nonhydrolytic colloidal routes. *Angew. Chemie - Int. Ed.* **45**, 3414–3439 (2006).
42. Wang, S., McGuirk, C. M., D'Aquino, A., Mason, J. A. & Mirkin, C. A. Metal–Organic Framework Nanoparticles. *Adv. Mater.* **30**, 1800202 (2018).
43. Patzke, G. R., Zhou, Y., Kontic, R. & Conrad, F. Oxide Nanomaterials: Synthetic Developments, Mechanistic Studies, and Technological Innovations. *Angew. Chemie Int. Ed.* **50**, 826–859 (2011).
44. Li, N., Zhao, P. & Astruc, D. Anisotropic gold nanoparticles: Synthesis, properties, applications, and toxicity. *Angew. Chemie Int. Ed.* **53**, 1756–1789 (2014).
45. Lisjak, D. & Mertelj, A. Anisotropic magnetic nanoparticles: A review of their properties, syntheses and potential applications. *Prog. Mater. Sci.* **95**, 286–328 (2018).
46. Wu, Z., Yang, S. & Wu, W. Shape control of inorganic nanoparticles from solution. *Nanoscale* **8**, 1237–1259 (2016).
47. Narayan, R., Nayak, U. Y., Raichur, A. M. & Garg, S. Mesoporous silica nanoparticles: A comprehensive review on synthesis and recent advances. *Pharmaceutics* **10**, 1–49 (2018).



48. Ma, W. *et al.* Chiral Inorganic Nanostructures. *Chem. Rev.* **117**, 8041–8093 (2017).
49. Thanh, N. T. K., Maclean, N. & Mahiddine, S. Mechanisms of nucleation and growth of nanoparticles in solution. *Chem. Rev.* **114**, 7610–7630 (2014).
50. Wall, M. A. *et al.* Surfactant-Free Shape Control of Gold Nanoparticles Enabled by Unified Theoretical Framework of Nanocrystal Synthesis. *Adv. Mater.* **29**, (2017).
51. Li, Y. & Shen, W. *Morphology-dependent nanocatalysts: Rod-shaped oxides.* *Chemical Society Reviews* **43**, (2014).
52. Soon, G. K. & Hyeon, T. Colloidal chemical synthesis and formation kinetics of uniformly sized nanocrystals of metals, oxides, and chalcogenides. *Acc. Chem. Res.* **41**, 1696–1709 (2008).
53. Yin, Y. & Alivisatos, A. P. Colloidal nanocrystal synthesis and the organic–inorganic interfac. *Nature* **437**, 664–670 (2005).
54. Hu, J. *et al.* Linearly Polarized Emission from Colloidal Semiconductor Quantum Rods. *Science (80-. ).* **292**, 2060–2064 (2001).
55. Feng, L., Wang, K., Powell, J. & Zhou, H. Controllable Synthesis of Metal-Organic Frameworks and Their Hierarchical Assemblies. *Matter* **1**, 801–824 (2019).
56. Kuijk, A., Blaaderen, A. Van & Imhof, A. Synthesis of Monodisperse, Rodlike Silica Colloids with Tunable Aspect Ratio. *J. Am. Chem. Soc.* **133**, 2346–2349 (2011).
57. Wu, W. *et al.* Growth of single crystal graphene arrays by locally controlling nucleation on polycrystalline Cu using chemical vapor deposition. *Adv. Mater.* **23**, 4898–4903 (2011).
58. Yu, Q. *et al.* Control and characterization of individual grains and grain boundaries in graphene grown by chemical vapour deposition. *Nat. Mater.* **10**, 443–449 (2011).
59. Ogi, S., Sugiyasu, K., Manna, S., Samitsu, S. & Takeuchi, M. Living supramolecular polymerization realized through a biomimetic approach. *Nat. Chem.* **6**, 188–195 (2014).
60. Kang, J. *et al.* A rational strategy for the realization of chain-growth supramolecular polymerization. *Science (80-. ).* **347**, 646–651 (2015).



61. Wang, X. *et al.* Cylindrical Block Copolymer Micelles and Co-Micelles of Controlled Length and Architecture. *Science* (80-. ). **317**, 644–648 (2007).
62. Qian, J. *et al.* Uniform, high aspect ratio fiber-like micelles and block co-micelles with a crystalline  $\pi$ -conjugated polythiophene core by self-seeding. *J. Am. Chem. Soc.* **136**, 4121–4124 (2014).
63. Qian, J. *et al.* Self-seeding in one dimension: A route to uniform fiber-like nanostructures from block copolymers with a crystallizable core-forming block. *ACS Nano* **7**, 3754–3766 (2013).
64. Xu, J. *et al.* Synergistic self-seeding in one-dimension: a route to patchy and block comicelles with uniform and controllable length. *Chem. Sci.* **10**, 2280–2284 (2019).
65. Qian, J. *et al.* Self-seeding in one dimension: An approach to control the length of fiberlike polyisoprene-polyferrocenylsilane block copolymer micelles. *Angew. Chemie - Int. Ed.* **50**, 1622–1625 (2011).
66. Inam, M. *et al.* 1D: Vs. 2D shape selectivity in the crystallization-driven self-assembly of polylactide block copolymers. *Chem. Sci.* **8**, 4223–4230 (2017).
67. He, X. *et al.* Two-dimensional assemblies from crystallizable homopolymers with charged termini. *Nat. Mater.* **16**, 481–488 (2017).
68. Qiu, H., Du, V. A., Winnik, M. A. & Manners, I. Branched cylindrical micelles via crystallization-driven self-assembly. *J. Am. Chem. Soc.* **135**, 17739–17742 (2013).
69. He, F., Gädt, T., Manners, I. & Winnik, M. A. Fluorescent ‘barcode’ multiblock co-micelles via the living self-assembly of di- and triblock copolymers with a crystalline core-forming metalloblock. *J. Am. Chem. Soc.* **133**, 9095–9103 (2011).
70. Wang, H. *et al.* Cylindrical block co-micelles with spatially selective functionalization by nanoparticles. *J. Am. Chem. Soc.* **129**, 12924–12925 (2007).
71. Arno, M. C. *et al.* Precision Epitaxy for Aqueous 1D and 2D Poly( $\epsilon$ -caprolactone) Assemblies. *J. Am. Chem. Soc.* **139**, 16980–16985 (2017).
72. Qiu, H. *et al.* Tunable supermicelle architectures from the hierarchical self-assembly of



- amphiphilic cylindrical B-A-B triblock Co-micelles. *Angew. Chemie - Int. Ed.* **51**, 11882–11885 (2012).
73. Pal, D. S., Kar, H. & Ghosh, S. Controllable Supramolecular Polymerization via Chain-growth Mechanism. *Chem. Commun.* **54**, 928–931 (2018).
74. Sasaki, N. *et al.* Supramolecular double-stranded Archimedean spirals and concentric toroids. *Nat. Commun.* **11**, 1–9 (2020).
75. *Foldamers: Structure, Properties and Applications.* (WILEY-VCH Verlag GmbH, 2007).
76. Frisch, H., Tuten, B. T. & Barner-Kowollik, C. Macromolecular Superstructures: A Future Beyond Single Chain Nanoparticles. *Isr. J. Chem.* **60**, 86–99 (2020).
77. Hanlon, A. M., Lyon, C. K. & Berda, E. B. What Is Next in Single-Chain Nanoparticles? *Macromolecules* **49**, 2–14 (2016).
78. Gonzalez-Burgos, M., Latorre-Sanchez, A. & Pomposo, J. A. Advances in single chain technology. *Chem. Soc. Rev.* **44**, 6122–6142 (2015).
79. Altintas, O. & Barner-Kowollik, C. Single-Chain Folding of Synthetic Polymers: A Critical Update. *Macromol. Rapid Commun.* **37**, 29–46 (2016).
80. Rubio-Cervilla, J., Frisch, H., Barner-Kowollik, C. & Pomposo, J. A. Synthesis of Single-Ring Nanoparticles Mimicking Natural Cyclotides by a Stepwise Folding-Activation-Collapse Process. *Macromol. Rapid Commun.* **40**, 1–6 (2019).
81. Zhang, J. *et al.* Self-assembly and disassembly of stimuli responsive tadpole-like single chain nanoparticles using a switchable hydrophilic/hydrophobic boronic acid cross-linker. *Polym. Chem.* **8**, 4079–4087 (2017).
82. Matsumoto, M., Sawamoto, M. & Terashima, T. Orthogonal Folding of Amphiphilic/Fluorous Random Block Copolymers for Double and Multicompartment Micelles in Water. *ACS Macro Lett.* **8**, 320–325 (2019).
83. Roy, R. K. & Lutz, J. F. Compartmentalization of single polymer chains by stepwise intramolecular cross-linking of sequence-controlled macromolecules. *J. Am. Chem. Soc.* **136**,



12888–12891 (2014).

84. Schmidt, B. V. K. J., Fechner, N., Falkenhagen, J. & Lutz, J. F. Controlled folding of synthetic polymer chains through the formation of positionable covalent bridges. *Nat. Chem.* **3**, 234–238 (2011).
85. Heguri, H., Yamamoto, T. & Tezuka, Y. Folding Construction of a Pentacyclic Quadruply fused Polymer Topology with Tailored kyklo-Telechelic Precursors. *Angew. Chemie - Int. Ed.* **54**, 8688–8692 (2015).
86. Devanand, K. & Selser, J. C. Asymptotic Behavior and Long-Range Interactions in Aqueous Solutions of Poly(ethylene oxide). *Macromolecules* **24**, 5943–5947 (1991).
87. Verduzco, R., Li, X., Pesek, S. L. & Stein, G. E. Structure, function, self-assembly, and applications of bottlebrush copolymers. *Chem. Soc. Rev.* **44**, 2405–2420 (2015).
88. Xie, G., Martinez, M. R., Olszewski, M., Sheiko, S. S. & Matyjaszewski, K. Molecular Bottlebrushes as Novel Materials. *Biomacromolecules* **20**, 27–54 (2019).
89. Seeman, N. C. Nucleic acid junctions and lattices. *J. Theor. Biol.* **99**, 237–247 (1982).
90. Rothemund, P. W. K. Folding DNA to create nanoscale shapes and patterns. *Nature* **440**, 297–302 (2006).
91. Ong, L. L. *et al.* Programmable self-assembly of three-dimensional nanostructures from 10,000 unique components. *Nat. Publ. Gr.* **552**, (2017).
92. Ke, Y., Ong, L. L., Shih, W. M. & Yin, P. Three-dimensional structures self-assembled from DNA bricks. *Science (80-. ).* **338**, 1177–1183 (2012).
93. Zhang, F. *et al.* Complex wireframe DNA origami nanostructures with multi-arm junction vertices. *Nat. Nanotechnol.* **10**, 779–784 (2015).
94. Praetorius, F. & Dietz, H. Biotechnological mass production of DNA origami. *Nature* **552**, 84–87 (2017).
95. Chen, Y. J., Groves, B., Muscat, R. A. & Seelig, G. DNA nanotechnology from the test tube to the cell. *Nat. Nanotechnol.* **10**, 748–760 (2015).



96. Luo, Q., Hou, C., Bai, Y., Wang, R. & Liu, J. Protein Assembly: Versatile Approaches to Construct Highly Ordered Nanostructures. *Chem. Rev.* **116**, 13571–13632 (2016).
97. Park, K. *et al.* Control of repeat-protein curvature by computational protein design. *Nat. Struct. Mol. Biol.* **22**, 167–174 (2015).
98. Bai, Y. *et al.* Highly ordered protein nanorings designed by accurate control of glutathione S-transferase self-assembly. *J. Am. Chem. Soc.* **135**, 10966–10969 (2013).
99. King, N. P. *et al.* Accurate design of co-assembling multi-component protein nanomaterials. *Nature* **510**, 103–108 (2014).
100. Gradišar, H. *et al.* Design of a single-chain polypeptide tetrahedron assembled from coiled-coil segments. *Nat. Chem. Biol.* **9**, 362–366 (2013).
101. Thomson, A. R. *et al.* Computational design of water-soluble  $\alpha$ -helical barrels. *Science (80-. )*. **346**, 485–488 (2014).
102. Huang, P. S. *et al.* High thermodynamic stability of parametrically designed helical bundles. *Science (80-. )*. **346**, 481–485 (2014).
103. Wagenbauer, K. F., Sigl, C. & Dietz, H. Gigadalton-scale shape-programmable DNA assemblies. *Nature* **552**, 78–83 (2017).
104. Yokoi, N. *et al.* Construction of robust bio-nanotubes using the controlled self-assembly of component proteins of bacteriophage T4. *Small* **6**, 1873–1879 (2010).
105. Ghosh Chaudhuri, R. & Paria, S. Core/shell nanoparticles: Classes, properties, synthesis mechanisms, characterization, and applications. *Chem. Rev.* **112**, 2373–2433 (2012).
106. Wang, X. *et al.* Biomineralization State of Viruses and Their Biological Potential. *Chem. - A Eur. J.* **24**, 11518–11529 (2018).
107. Butler, P. J. G. Self-assembly of tobacco mosaic virus: The role of an intermediate aggregate in generating both specificity and speed. *Philos. Trans. R. Soc. B Biol. Sci.* **354**, 537–550 (1999).
108. Shukla, S. *et al.* The impact of aspect ratio on the biodistribution and tumor homing of rigid



- soft-matter nanorods. *Adv. Healthc. Mater.* **4**, 874–882 (2015).
109. Dujardin, E., Peet, C., Stubbs, G., Culver, J. N. & Mann, S. Organization of metallic nanoparticles using tobacco mosaic virus templates. *Nano Lett.* **3**, 413–417 (2003).
  110. Fowler, C. E., Shenton, W., Stubbs, G. & Mann, S. Tobacco mosaic virus liquid crystals as templates for the interior design of silica mesophases and nanoparticles. *Adv. Mater.* **13**, 1266–1269 (2001).
  111. Shenton, W., Douglas, T., Young, M., Stubbs, G. & Mann, S. Inorganic-organic nanotube composites from template mineralization of tobacco mosaic virus. *Adv. Mater.* **11**, 253–256 (1999).
  112. Saunders, K. & Lomonosoff, G. P. In planta synthesis of designer-length tobacco mosaic virus-based nano-rods that can be used to fabricate nano-wires. *Front. Plant Sci.* **8**, 1–11 (2017).
  113. Liu, X. *et al.* Complex silica composite nanomaterials templated with DNA origami. *Nature* **559**, 593–598 (2018).
  114. Nguyen, L., Döblinger, M., Liedl, T. & Heuer-Jungemann, A. DNA-Origami-Templated Silica Growth by Sol–Gel Chemistry. *Angew. Chemie - Int. Ed.* **58**, 912–916 (2019).
  115. Liu, X. *et al.* DNA Framework-Encoded Mineralization of Calcium Phosphate. *Chem* **6**, 472–485 (2020).
  116. Ma, N. *et al.* *Directional Assembly of Nanoparticles by DNA Shapes: Towards Designed Architectures and Functionality. Topics in Current Chemistry* **378**, (Springer International Publishing, 2020).
  117. Chen, Z., Liu, C., Cao, F., Ren, J. & Qu, X. DNA metallization: Principles, methods, structures, and applications. *Chem. Soc. Rev.* **47**, 4017–4072 (2018).
  118. Li, N. *et al.* Fabrication of Metal Nanostructures on DNA Templates. *ACS Appl. Mater. Interfaces* **11**, 13835–13852 (2019).
  119. Dong, Y. *et al.* Cuboid Vesicles Formed by Frame-Guided Assembly on DNA Origami



Scaffolds. *Angew. Chemie Int. Ed.* (2016). doi:10.1002/anie.201610133

120. Ji, H. *et al.* Improvement in Crystallinity and Porosity of Poorly Crystalline Metal-Organic Frameworks (MOFs) through Their Induced Growth on a Well-Crystalline MOF Template. *Inorg. Chem.* **57**, 9048–9054 (2018).
121. Zhou, K. & Qiangbin, W. Nanowires and Nanoparticle Chains Inside Tubular Viral Templates. in *Virus-Derived Nanoparticles for Advanced Technologies. Methods in Molecular Biology*, vol 1776 (Humana Press, 2018).
122. Helmi, S., Ziegler, C., Kauert, D. J. & Seidel, R. Shape-controlled synthesis of gold nanostructures using DNA origami molds. *Nano Lett.* **14**, 6693–6698 (2014).
123. Sun, W. *et al.* Casting inorganic structures with DNA molds. *Science (80-. ).* **346**, (2014).
124. Bayrak, T. *et al.* DNA-Mold Templated Assembly of Conductive Gold Nanowires. *Nano Lett.* **18**, 2116–2123 (2018).
125. Ye, J., Helmi, S., Teske, J. & Seidel, R. Fabrication of Metal Nanostructures with Programmable Length and Patterns Using a Modular DNA Platform. *Nano Lett.* **19**, 2707–2714 (2019).
126. Dong, Y. & Mao, Y. DNA Origami as Scaffolds for Self-Assembly of Lipids and Proteins. *ChemBioChem* **20**, 2422–2431 (2019).
127. Zhang, Z., Yang, Y., Pincet, F., Llaguno, M. C. & Lin, C. Placing and shaping liposomes with reconfigurable DNA nanocages. *Nat. Chem.* **9**, 653–659 (2017).
128. Tokura, Y. *et al.* Polymer tube nanoreactors: Via DNA-origami templated synthesis. *Chem. Commun.* **54**, 2808–2811 (2018).
129. Li, N. *et al.* Precise Organization of Metal and Metal Oxide Nanoclusters into Arbitrary Patterns on DNA Origami. *J. Am. Chem. Soc.* **141**, 17968–17972 (2019).
130. Shang, Y. *et al.* Site-Specific Synthesis of Silica Nanostructures on DNA Origami Templates. *Adv. Mater.* **32**, 2000294 (2020).
131. Kim, F. *et al.* Functionalized DNA nanostructures as scaffolds for guided mineralization.



- Chem. Sci.* **10**, 10537–10542 (2019).
132. Luo, X., Lachance-Brais, C., Bantle, A. & Sleiman, H. F. The assemble, grow and lift-off (AGLO) strategy to construct complex gold nanostructures with pre-designed morphologies. *Chem. Sci.* 4911–4921 (2020). doi:10.1039/d0sc00553c
  133. Tokura, Y. *et al.* Fabrication of Defined Polydopamine Nanostructures by DNA Origami-Templated Polymerization. *Angew. Chemie - Int. Ed.* **57**, 1587–1591 (2018).
  134. Tokura, Y. *et al.* Bottom-Up Fabrication of Nanopatterned Polymers on DNA Origami by In Situ Atom-Transfer Radical Polymerization. *Angew. Chem. Int. Ed. Engl.* **55**, 5692–5697 (2016).
  135. Burrows, N. D. *et al.* Anisotropic Nanoparticles and Anisotropic Surface Chemistry. *J. Phys. Chem. Lett.* **7**, 632–641 (2016).
  136. El-sayed, M. A. Some Interesting Properties of Metals Confined in Time and Nanometer Space of Different Shapes. *Acc. Chem. Res.* **34**, 257–264 (2001).
  137. Zande, B. M. I. Van Der, Bo, M. R., Fokkink, L. G. J. & Schonenberger, C. Aqueous Gold Sols of Rod-Shaped Particles. *J. Phys. Chem. B* **101**, 852–854 (1997).
  138. Yu, Y., Chang, S., Lee, C. & Wang, C. R. C. Gold Nanorods : Electrochemical Synthesis and Optical Properties. *J. Phys. Chem. B* **101**, 6661–6664 (1997).
  139. Lee, K. & El-sayed, M. A. Gold and Silver Nanoparticles in Sensing and Imaging : Sensitivity of Plasmon Response to Size , Shape , and Metal Composition. *J. Phys. Chem. B* **110**, 19220–19225 (2006).
  140. Mayer, K. M. & Hafner, J. H. Localized Surface Plasmon Resonance Sensors. *Chem. Rev.* **111**, 3828–3857 (2011).
  141. Hu, M. *et al.* Gold nanostructures : engineering their plasmonic properties for biomedical applications. *Chem. Soc. Rev.* **35**, 1084–1094 (2006).
  142. Bedford, E. E., Spadavecchia, J., Pradier, C. & Gu, F. X. Surface Plasmon Resonance Biosensors Incorporating Gold Nanoparticles. *Macromol. Biosci.* **12**, 724–739 (2012).



143. Zijlstra, P., Paulo, P. M. R. & Orrit, M. Optical detection of single non-absorbing molecules using the surface plasmon resonance of a gold nanorod. *Nat. Nanotechnol.* **7**, 379–382 (2012).
144. Ament, I., Prasad, J., Henkel, A., Schmachtel, S. & Sönnichsen, C. Single unlabeled protein detection on individual plasmonic nanoparticles. *Nano Lett.* **12**, 1092–1095 (2012).
145. Huang, X., El-Sayed, I. H., Qian, W. & El-Sayed, M. A. Cancer cell imaging and photothermal therapy in the near-infrared region by using gold nanorods. *J. Am. Chem. Soc.* **128**, 2115–2120 (2006).
146. Mock, J. J., Barbic, M., Schultz, D. A. & Schultz, S. Shape effects in plasmon resonance of individual colloidal silver nanoparticles. *J. Chem. Phys.* **116**, 6755–6759 (2005).
147. Sau, T. K. & Murphy, C. J. Seeded High Yield Synthesis of Short Au Nanorods in Aqueous Solution. *Langmuir* **20**, 6414–6420 (2004).
148. Wu, H. L., Chen, C. H. & Huang, M. H. Seed-mediated synthesis of branched gold nanocrystals derived from the side growth of pentagonal bipyramids and the formation of gold nanostars. *Chem. Mater.* **21**, 110–114 (2009).
149. Yuan, H. *et al.* Gold nanostars: Surfactant-free synthesis, 3D modelling, and two-photon photoluminescence imaging. *Nanotechnology* **23**, 075102 (2012).
150. Millstone, J. E. *et al.* Observation of a quadrupole plasmon mode for a colloidal solution of gold nanoprisms. *J. Am. Chem. Soc.* **127**, 5312–5313 (2005).
151. Schatz, G. C. Theoretical Studies of Surface Enhanced Raman Scattering. *Acc. Chem. Res.* **17**, 370–376 (1984).
152. Reguera, J., Langer, J., Jimenez de Aberasturi, D. & Liz-marzan, L. M. Anisotropic metal nanoparticles for surface enhanced Raman scattering. *Chem. Soc. Rev.* **46**, 3866–3885 (2017).
153. Harmsen, S. *et al.* Surface-enhanced resonance Raman scattering nanostars for high-precision cancer imaging. *Sci. Transl. Med.* **7**, 271ra7-271ra7 (2015).



154. Dong, Y. *et al.* Controlling Anisotropy of Quantum-Confined CsPbBr<sub>3</sub> Nanocrystals by Combined Use of Equilibrium and Kinetic Anisotropy. *Chem. Mater.* **31**, 5655–5662 (2019).
155. Gu, L. *et al.* A biomimetic eye with a hemispherical perovskite nanowire array retina. *Nature* **581**, 278–282 (2020).
156. Ferry, D. K., Goodnick, S. M. & Bird, J. *Transport in Nanostructures*. *Transport in Nanostructures* (Cambridge University Press, 2009). doi:10.1017/CBO9780511840463
157. Burda, C., Chen, X., Narayanan, R. & El-Sayed, M. A. *Chemistry and properties of nanocrystals of different shapes*. *Chemical Reviews* **105**, (2005).
158. Zhang, Q., Uchaker, E., Candelaria, S. L. & Cao, G. Nanomaterials for energy conversion and storage. *Chem. Soc. Rev.* **42**, 3127–3171 (2013).
159. Aricò, A. S. *et al.* Nanostructured materials for advanced energy conversion and storage devices. *Nat. Mater.* **4**, 366–377 (2005).
160. Quan, L. N., Kang, J., Ning, C. & Yang, P. Nanowires for Photonics. *Chem. Rev.* **119**, 9153–9169 (2019).
161. Yan, R., Gargas, D. & Yang, P. Nanowire photonics. *Nat. Photonics* **3**, 569–576 (2009).
162. Eaton, S. W., Fu, A., Wong, A. B., Ning, C.-Z. & Yang, P. Semiconductor Nanowire Lasers. *Nat. Rev. Mater.* **1**, 16028 (2016).
163. Zhou, Z. J. *et al.* Effect of highly ordered single-crystalline TiO<sub>2</sub> nanowire length on the photovoltaic performance of dye-sensitized solar cells. *ACS Appl. Mater. Interfaces* **3**, 4349–4353 (2011).
164. Leschkies, K. S., Jacobs, A. G., Norris, D. J. & Aydil, E. S. Nanowire-quantum-dot solar cells and the influence of nanowire length on the charge collection efficiency. *Appl. Phys. Lett.* **95**, 2007–2010 (2009).
165. Law, M., Greene, L. E., Johnson, J. C., Saykally, R. & Yang, P. Nanowire dye-sensitized solar cells. *Nat. Mater.* **4**, 455–459 (2005).
166. Liu, J. *et al.* Length-independent charge transport of well-separated single-crystal TiO<sub>2</sub> long



- nanowire arrays. *Chem. Sci.* **9**, 7400–7404 (2018).
167. Jin, X. *et al.* Long-range exciton transport in conjugated polymer nanofibers prepared by seeded growth. *Science* (80-. ). **360**, 897–900 (2018).
  168. Narayanan, R. & El-Sayed, M. A. Shape-dependent catalytic activity of platinum nanoparticles in colloidal solution. *Nano Lett.* **4**, 1343–1348 (2004).
  169. Rashid, M. H. & Mandal, T. K. Templateless synthesis of polygonal gold nanoparticles: An unsupported and reusable catalyst with superior activity. *Adv. Funct. Mater.* **18**, 2261–2271 (2008).
  170. Xu, R., Wang, D., Zhang, J. & Li, Y. Shape-dependent catalytic activity of silver nanoparticles for the oxidation of styrene. *Chem. - An Asian J.* **1**, 888–893 (2006).
  171. Mahmoud, M. A., Tabor, C. E., El-Sayed, M. A., Ding, Y. & Zhong, L. W. A new catalytically active colloidal platinum nanocatalyst: The multiarmed nanostar single crystal. *J. Am. Chem. Soc.* **130**, 4590–4591 (2008).
  172. Lim, B. *et al.* Facile synthesis of highly faceted multioctahedral Pt nanocrystals through controlled overgrowth. *Nano Lett.* **8**, 4043–4047 (2008).
  173. Gong, X. *et al.* Controlled synthesis of Pt nanoparticles via seeding growth and their shape-dependent catalytic activity. *J. Colloid Interface Sci.* **352**, 379–385 (2010).
  174. Li, X. *et al.* The unusual effect of AgNO<sub>3</sub> on the growth of Au nanostructures and their catalytic performance. *Nanoscale* **5**, 4976–4985 (2013).
  175. Sanles-Sobrido, M. *et al.* Highly catalytic single-crystal dendritic pt nanostructures supported on carbon nanotubes. *Chem. Mater.* **21**, 1531–1535 (2009).
  176. Fontaíña-Troitiño, N. *et al.* Room-temperature ferromagnetism in antiferromagnetic cobalt oxide nanooctahedra. *Nano Lett.* **14**, 640–647 (2014).
  177. Murphy, C. J. & Jana, N. R. Controlling the aspect ratio of inorganic nanorods and nanowires. *Adv. Mater.* **14**, 80–82 (2002).
  178. Lee, S. M., Cho, S. N. & Cheon, J. Anisotropic shape control of colloidal inorganic



- nanocrystals. *Adv. Mater.* **15**, 441–444 (2003).
179. Park, S. J. *et al.* Synthesis and magnetic studies of uniform iron nanorods and nanospheres [12]. *J. Am. Chem. Soc.* **122**, 8581–8582 (2000).
  180. Wang, C., Hou, Y., Kim, J. & Sun, S. A general strategy for synthesizing FePt nanowires and nanorods. *Angew. Chemie - Int. Ed.* **46**, 6333–6335 (2007).
  181. Chen, M. *et al.* Synthesis and self-assembly of fcc phase FePt nanorods. *J. Am. Chem. Soc.* **129**, 6348–6349 (2007).
  182. Du, Y. P., Zhang, Y. W., Sun, L. D. & Yan, C. H. Self-assembled ferromagnetic monodisperse manganese oxide nanoplates synthesized by a modified nonhydrolytic approach. *J. Phys. Chem. C* **113**, 6521–6528 (2009).
  183. Dumestre, F. *et al.* Shape Control of Thermodynamically Stable Cobalt Nanorods through Organometallic Chemistry. *Angew. Chemie - Int. Ed.* **41**, 4286–4289 (2002).
  184. Dumestre, F. *et al.* Unprecedented Crystalline Super-Lattices of Monodisperse Cobalt Nanorods. *Angew. Chemie - Int. Ed.* **41**, 4286–4289 (2002).
  185. Di Paola, C., D'Agosta, R. & Baletto, F. Geometrical Effects on the Magnetic Properties of Nanoparticles. *Nano Lett.* **16**, 2885–2889 (2016).
  186. Zhang, H. T., Ding, J. & Chow, G. M. Morphological control of synthesis and anomalous magnetic properties of 3-D branched Pt nanoparticles. *Langmuir* **24**, 375–378 (2008).
  187. Yuan, J. *et al.* Synthesis of ZnO-Pt nanoflowers and their photocatalytic applications. *Nanotechnology* **21**, 10 (2010).
  188. Wei, Q. *et al.* Gyromagnetic imaging: Dynamic optical contrast using gold nanostars with magnetic cores. *J. Am. Chem. Soc.* **131**, 9728–9734 (2009).
  189. Wang, M. *et al.* Magnetic tuning of plasmonic excitation of gold nanorods. *J. Am. Chem. Soc.* **135**, 15302–15305 (2013).
  190. Wang, M., He, L., Zorba, S. & Yin, Y. Magnetically actuated liquid crystals. *Nano Lett.* **14**, 3966–3971 (2014).



191. Wang, M., He, L., Xu, W., Wang, X. & Yin, Y. Magnetic Assembly and Field-Tuning of Ellipsoidal-Nanoparticle-Based Colloidal Photonic Crystals. *Angew. Chemie - Int. Ed.* **54**, 7077–7081 (2015).
192. Kumar, A., Kumar, A. & Rai, A. Rheological behaviour of nanofluids: A review. *Renew. Sustain. Energy Rev.* **53**, 779–791 (2016).
193. Murshed, S. M. S. & Estellé, P. A state of the art review on viscosity of nanofluids. *Renew. Sustain. Energy Rev.* **76**, 1134–1152 (2017).
194. Abraham, J., Sharika, T., Mishra, R. K. & Thomas, S. *14 - Rheological characteristics of nanomaterials and nanocomposites. Micro and Nano Fibrillar Composites (MFCs and NFCs) from Polymer Blends* (Elsevier Ltd., 2017). doi:10.1016/B978-0-08-101991-7.00014-5
195. Cherkasova, A. S. & Shan, J. W. Particle Aspect-Ratio and Agglomeration-State Effects on the Effective Thermal Conductivity of Aqueous Suspensions of Multiwalled Carbon Nanotubes. *J. Heat Transfer* **132**, (2010).
196. Jabbari-farouji, S., Weis, J., Davidson, P., Levitz, P. & Trizac, E. Interplay of anisotropy in shape and interactions in charged platelet suspensions platelet suspensions. *J. Chem. Phys.* **141**, 224510 (2014).
197. Brown, A. B. D., Clarke, S. M., Convert, P. & Rennie, A. R. Orientational order in concentrated dispersions of plate-like kaolinite particles under shear. *J. Rheol. (N. Y. N. Y.)* **44**, 221–233 (2000).
198. Xu, J., Chatterjee, S., Koelling, K. W., Wang, Y. & Bechtel, S. E. Shear and extensional rheology of carbon nanofiber suspensions. *Rheol. Acta* **44**, 537–562 (2005).
199. Brown, A. B. D., Clarke, S. M., Convert, P. & Rennie, A. R. Orientational order in concentrated dispersions of plate-like kaolinite particles under shear. *J. Rheol. (N. Y. N. Y.)* **44**, 221–233 (2000).
200. Boo, W. *et al.* Effect of nanoplatelet aspect ratio on mechanical properties of epoxy nanocomposites. *Polymer (Guildf)*. **48**, 1075–1082 (2007).



201. White, K. L., Hawkins, S., Miyamoto, M., Takahara, A. & Sue, H.-J. Effects of aspect ratio and concentration on rheology of epoxy suspensions containing model plate- like nanoparticles. *Phys. Fluids* **27**, 123306 (2015).
202. Ye, X., Kandlikar, S. G. & Li, C. Viscosity of nanofluids containing anisotropic particles: A critical review and a comprehensive model. *European Physical Journal E* **42**, (2019).
203. Förster, S., Konrad, M. & Lindner, P. Shear thinning and orientational ordering of Wormlike Micelles. *Phys. Rev. Lett.* **94**, (2005).
204. Simon, K. A. *et al.* Disulfide-Based Diblock Copolymer Worm Gels: A Wholly-Synthetic Thermoreversible 3D Matrix for Sheet-Based Cultures. *Biomacromolecules* **16**, 3952–3958 (2015).
205. Warren, N. J., Rosselgong, J., Madsen, J. & Armes, S. P. Disulfide-Functionalized Diblock Copolymer Worm Gels. *Biomacromolecules* **16**, 2514–2521 (2015).
206. Matter, F., Luna, A. L. & Niederberger, M. From colloidal dispersions to aerogels: How to master nanoparticle gelation. *Nano Today* **30**, 100827 (2020).
207. Prince, E. *et al.* Patterning of Structurally Anisotropic Composite Hydrogel Sheets. *Biomacromolecules* **19**, 1276–1284 (2018).
208. Diba, M., Polini, A., Petre, D. G., Zhang, Y. & Leeuwenburgh, S. C. G. Fiber-reinforced colloidal gels as injectable and moldable biomaterials for regenerative medicine. *Mater. Sci. Eng. C* **92**, 143–150 (2018).
209. Beck-Candanedo, S., Roman, M. & Gray, D. G. Effect of Reaction Conditions on the Properties and Behavior of Wood Cellulose Nanocrystal Suspensions. *Biomacromolecules* **6**, 1048–1054 (2005).
210. Sacui, I. A. *et al.* Comparison of the properties of cellulose nanocrystals and cellulose nanofibrils isolated from bacteria, tunicate, and wood processed using acid, enzymatic, mechanical, and oxidative methods. *ACS Appl. Mater. Interfaces* **6**, 6127–6138 (2014).
211. Yang, J., Han, C.-R., Zhang, X.-M., Xu, F. & Sun, R.-C. Cellulose Nanocrystals Mechanical



- Reinforcement in Composite Hydrogels with Multiple Cross-Links: Correlations between Dissipation Properties and Deformation Mechanisms. *Macromolecules* **47**, 4077–4086 (2014).
212. McKee, J. R. *et al.* Thermoresponsive Nanocellulose Hydrogels with Tunable Mechanical Properties. *ACS Macro Lett.* **3**, 266–270 (2014).
  213. Chau, M. *et al.* Composite Hydrogels with Tunable Anisotropic Morphologies and Mechanical Properties. *Chem. Mater.* **28**, 3406–3415 (2016).
  214. McKee, J. R. *et al.* Healable, Stable and Stiff Hydrogels: Combining Conflicting Properties Using Dynamic and Selective Three-Component Recognition with Reinforcing Cellulose Nanorods. *Adv. Funct. Mater.* **24**, 2706–2713 (2014).
  215. Siqueira, G. *et al.* Cellulose Nanocrystal Inks for 3D Printing of Textured Cellular Architectures. *Adv. Funct. Mater.* **27**, 1604619 (2017).
  216. Kam, D. *et al.* Direct Cryo Writing of Aerogels Via 3D Printing of Aligned Cellulose Nanocrystals Inspired by the Plant Cell Wall. *Colloids and Interfaces* **3**, 46 (2019).
  217. Sultan, S. & Mathew, A. P. 3D printed scaffolds with gradient porosity based on a cellulose nanocrystal hydrogel. *Nanoscale* **10**, 4421–4431 (2018).
  218. Yang, J. & Han, C. Mechanically Viscoelastic Properties of Cellulose Nanocrystals Skeleton Reinforced Hierarchical Composite Hydrogels. *ACS Appl. Mater. Interfaces* **8**, 25621–25630 (2016).
  219. De France, K. J. *et al.* 2.5D Hierarchical Structuring of Nanocomposite Hydrogel Films Containing Cellulose Nanocrystals. *ACS Appl. Mater. Interfaces* (2019). doi:10.1021/acsami.8b16232
  220. De France, K. J., Hoare, T. & Cranston, E. D. Review of Hydrogels and Aerogels Containing Nanocellulose. *Chem. Mater.* **29**, 4609–4631 (2017).
  221. De France, K. J., Cranston, E. D. & Hoare, T. Mechanically Reinforced Injectable Hydrogels. *ACS Appl. Polym. Mater.* **2**, 1016–1030 (2020).



222. Wang, K., Nune, K. C. & Misra, R. D. K. The functional response of alginate-gelatin-nanocrystalline cellulose injectable hydrogels toward delivery of cells and bioactive molecules. *Acta Biomater.* **36**, 143–151 (2016).
223. You, J. *et al.* Improved Mechanical Properties and Sustained Release Behavior of Cationic Cellulose Nanocrystals Reinforced Cationic Cellulose Injectable Hydrogels. *Biomacromolecules* **17**, 2839–2848 (2016).
224. Cunningham, V. J. *et al.* Tuning the critical gelation temperature of thermo-responsive diblock copolymer worm gels. *Polym. Chem.* **5**, 6307–6317 (2014).
225. Arno, M. C. *et al.* Exploiting the role of nanoparticle shape in enhancing hydrogel adhesive and mechanical properties. *Nat. Commun.* **11**, 1–9 (2020).
226. Keating, C. D. Aqueous Phase Separation as a Possible Route to Compartmentalization of Biological Molecules. *Acc. Chem. Res.* **45**, 2114–2124 (2012).
227. Hatti-Kaul, R. & Hatti-Kaul, R. Aqueous Two-Phase Systems: Methods and Protocols. in *Aqueous Two-Phase Systems* 1–10 (Humana Press, 2003). doi:10.1385/1592590284
228. Frith, W. J. Mixed biopolymer aqueous solutions - Phase behaviour and rheology. *Advances in Colloid and Interface Science* **161**, 48–60 (2010).
229. Chen, J., Spear, S. K., Huddleston, J. G. & Rogers, R. D. Polyethylene glycol and solutions of polyethylene glycol as green reaction media. *Green Chem.* **7**, 64–82 (2005).
230. Raja, S., Murty, V. R., Thivaharan, V., Rajasekar, V. & Ramesh, V. Aqueous Two Phase Systems for the Recovery of Biomolecules – A Review. *Sci. Technol.* **1**, 7–16 (2012).
231. Berton-Carabin, C. C. & Schroën, K. Pickering Emulsions for Food Applications: Background, Trends, and Challenges. *Annu. Rev. Food Sci. Technol.* **6**, 263–297 (2015).
232. Lagaly, G., Reese, M. & Abend, S. Smectites as colloidal stabilizers of emulsions: II. Rheological properties of smectite-laden emulsions. *Appl. Clay Sci.* **14**, 279–298 (1999).
233. Lagaly, G., Reese, M. & Abend, S. Smectites as colloidal stabilizers of emulsions I. Preparation and properties of emulsions with smectites and nonionic surfactants. *Appl. Clay*



- Sci.* **14**, 83–103 (1999).
234. Liang, F. *et al.* Inorganic Janus Nanosheets. *Angew. Chemie Int. Ed.* **50**, 2379–2382 (2011).
  235. Mejia, A. F. *et al.* Pickering emulsions stabilized by amphiphilic nano-sheets. *Soft Matter* **8**, 10245–10253 (2012).
  236. Loudet, J. C., Alsayed, A. M., Zhang, J. & Yodh, A. G. Capillary interactions between anisotropic colloidal particles. *Phys. Rev. Lett.* **94**, 18301 (2005).
  237. Loudet, J. C., Yodh, A. G. & Pouligny, B. Wetting and contact lines of micrometer-sized ellipsoids. *Phys Rev Lett* **97**, 18304 (2006).
  238. Lehle, H., Noruzifar, E. & Oettel, M. Ellipsoidal particles at fluid interfaces. *Eur. Phys. J. E* **26**, 151–160 (2008).
  239. Madivala, B., Fransaer, J. & Vermant, J. Self-Assembly and Rheology of Ellipsoidal Particles at Interfaces. *Langmuir* **25**, 2718–2728 (2009).
  240. Madivala, B., Vandebriel, S., Fransaer, J. & Vermant, J. Exploiting particle shape in solid stabilized emulsions. *Soft Matter* **5**, 1717–1727 (2009).
  241. Gomez-Flores, A., Bradford, S. A., Wu, L. & Kim, H. Interaction energies for hollow and solid cylinders: Role of aspect ratio and particle orientation. *Colloids Surfaces A* **580**, 123781 (2019).
  242. Inam, M. *et al.* Controlling the size of two-dimensional polymer platelets for water-in-water emulsifiers. *ACS Cent. Sci.* **4**, 63–70 (2018).
  243. Vis, M. *et al.* Water-in-Water Emulsions Stabilized by Nanoplates. *ACS Macro Lett.* **4**, 965–968 (2015).
  244. Peddireddy, K. R., Nicolai, T., Benyahia, L. & Capron, I. Stabilization of Water-in-Water Emulsions by Nanorods. *ACS Macro Lett.* **5**, 283–286 (2016).
  245. Kalashnikova, I., Bizot, H., Bertoncini, P., Cathala, B. & Capron, I. Cellulosic nanorods of various aspect ratios for oil in water Pickering emulsions. *Soft Matter* **9**, 952–959 (2013).
  246. Gratton, S. E. A. *et al.* The effect of particle design on cellular internalization pathways. *Proc.*



*Natl. Acad. Sci.* **105**, 11613–11618 (2008).

- 247. Kolhar, P. *et al.* Using shape effects to target antibody-coated nanoparticles to lung and brain endothelium. *Proc. Natl. Acad. Sci. U. S. A.* **110**, 10753–10758 (2013).
- 248. Bidan, C. M. *et al.* Geometry as a Factor for Tissue Growth: Towards Shape Optimization of Tissue Engineering Scaffolds. *Adv. Healthc. Mater.* **2**, 186–194 (2013).
- 249. Ruthardt, N., Lamb, D. C. & Bräuchle, C. Single-particle tracking as a quantitative microscopy-based approach to unravel cell entry mechanisms of viruses and pharmaceutical nanoparticles. *Mol. Ther.* **19**, 1199–1211 (2011).
- 250. Chithrani, B. D. & Chan, W. C. W. Elucidating the mechanism of cellular uptake and removal of protein-coated gold nanoparticles of different sizes and shapes. *Nano Lett.* **7**, 1542–1550 (2007).
- 251. Jiang, W., Kim, B. Y. S., Rutka, J. T. & Chan, W. C. W. Nanoparticle-mediated cellular response is size-dependent. *Nat. Nanotechnol.* **3**, 145–150 (2008).
- 252. Toy, R., Peiris, P. M., Ghaghada, K. B. & Karathanasis, E. The effect of particle size and shape on the in vivo journey of nanoparticles. *Futur. Med.* **9**, 121–134 (2014).
- 253. Geng, Y. *et al.* Shape effects of filaments versus spherical particles in flow and drug delivery. *Nat. Nanotechnol.* **2**, 249–255 (2007).
- 254. Chauhan, V. P. *et al.* Fluorescent nanorods and nanospheres for real-time in vivo probing of nanoparticle shape-dependent tumor penetration. *Angew Chem Int Ed* **50**, 11417–11420 (2011).
- 255. Xiong, F. *et al.* Superparamagnetic anisotropic nano-assemblies with longer blood circulation: In vivo: A highly efficient drug delivery carrier for leukemia therapy. *Nanoscale* **8**, 17085–17089 (2016).
- 256. Agarwal, R. *et al.* Mammalian cells preferentially internalize hydrogel nanodiscs over nanorods and use shape-specific uptake mechanisms. *Proc. Natl. Acad. Sci. U. S. A.* **110**, 17247–17252 (2013).



257. Alhmoud, H. *et al.* Porous silicon nanodiscs for targeted drug delivery. *Adv. Funct. Mater.* **25**, 1137–1145 (2015).
258. Lee, T. R. *et al.* On the near-wall accumulation of injectable particles in the microcirculation: Smaller is not better. *Sci. Rep.* **3**, (2013).
259. Godin, B. *et al.* Discoidal porous silicon particles: Fabrication and biodistribution in breast cancer bearing mice. *Adv. Funct. Mater.* **22**, 4225–4235 (2012).
260. Alemdaroglu, F. E., Alemdaroglu, N. C., Langguth, P. & Herrmann, A. Cellular uptake of DNA block copolymer micelles with different shapes. *Macromol. Rapid Commun.* **29**, 326–329 (2008).
261. Xu, X. H. N., Chen, J., Jeffers, R. B. & Kyriacou, S. Direct Measurement of Sizes and Dynamics of Single Living Membrane Transporters Using Nanooptics. *Nano Lett.* **2**, 175–182 (2002).
262. Qiu, H. *et al.* Uniform patchy and hollow rectangular platelet micelles from crystallizable polymer blends. *Science (80-. ).* **352**, 697–702 (2016).
263. Hudson, Z. M. *et al.* Tailored hierarchical micelle architectures using living crystallization-driven self-assembly in two dimensions. *Nat. Chem.* **6**, 893–898 (2014).
264. He, X. *et al.* Complex and Hierarchical 2D Assemblies via Crystallization-Driven Self-Assembly of Poly(l -lactide) Homopolymers with Charged Termini. *J. Am. Chem. Soc.* **139**, 9221–9228 (2017).
265. Nazemi, A. *et al.* Uniform ‘patchy’ Platelets by Seeded Heteroepitaxial Growth of Crystallizable Polymer Blends in Two Dimensions. *J. Am. Chem. Soc.* **139**, 4409–4417 (2017).
266. Lunn, D. J., Finnegan, J. R. & Manners, I. Self-assembly of ‘patchy’ nanoparticles: A versatile approach to functional hierarchical materials. *Chem. Sci.* **6**, 3663–3673 (2015).
267. Qiu, H., Hudson, Z. M., Winnik, M. A. & Manners, I. Multidimensional hierarchical self-assembly of amphiphilic cylindrical block comicelles. *Science (80-. ).* **347**, 1329–1332 (2015).



268. Li, Z. *et al.* Shape Effect of Glyco-Nanoparticles on Macrophage Cellular Uptake and Immune Response. *ACS Macro Lett.* **5**, 1059–1064 (2016).
269. Li, Z. *et al.* Glyco-Platelets with Controlled Morphologies via Crystallization-Driven Self-Assembly and Their Shape-Dependent Interplay with Macrophages. *ACS Macro Lett.* 596–602 (2019). doi:10.1021/acsmacrolett.9b00221
270. Inam, M. *et al.* Size and shape affects the antimicrobial activity of quaternized nanoparticles. *J. Polym. Sci. Part A Polym. Chem.* **57**, 255–259 (2019).
271. Decuzzi, P. *et al.* Size and shape effects in the biodistribution of intravascularly injected particles. *J. Control. Release* **141**, 320–327 (2010).
272. Van De Ven, A. L. *et al.* Rapid tumortropic accumulation of systemically injected plateloid particles and their biodistribution. *J. Control. Release* **158**, 148–155 (2012).
273. García-álvarez, R., Hadjidemetriou, M., Sánchez-iglesias, A., Liz-marzán, L. M. & Kostarelos, K. In vivo formation of protein corona on gold nanoparticles. The effect of their size and shape. *Nanoscale* **10**, 1256–1264 (2018).
274. Ou, Z., Wang, Z., Luo, B., Luijten, E. & Chen, Q. Kinetic pathways of crystallization at the nanoscale. *Nat. Mater.* **19**, 450–455 (2020).
275. Qin, W. *et al.* Microbe-Mediated Extracellular and Intracellular Mineralization: Environmental, Industrial, and Biotechnological Applications. *Adv. Mater.* **32**, (2020).
276. Nudelman, F. & Sommerdijk, N. A. J. M. Biomineralization as an inspiration for materials chemistry. *Angew. Chemie - Int. Ed.* **51**, 6582–6596 (2012).
277. Rawlings, A. E. *et al.* Artificial coiled coil biomineralisation protein for the synthesis of magnetic nanoparticles. *Nat. Commun.* **10**, (2019).
278. Chiu, C. Y. *et al.* Platinum nanocrystals selectively shaped using facet-specific peptide sequences. *Nat. Chem.* **3**, 393–399 (2011).
279. Rawlings, A. E. *et al.* Phage display selected magnetite interacting Adhirons for shape controlled nanoparticle synthesis. *Chem. Sci.* **6**, 5586–5594 (2015).



280. Wu, J. *et al.* DNA sequence-dependent morphological evolution of silver nanoparticles and their optical and hybridization properties. *J. Am. Chem. Soc.* **136**, 15195–15202 (2014).
281. Wang, Z., Tang, L., Tan, L. H., Li, J. & Lu, Y. Discovery of the DNA ‘genetic code’ for abiological gold nanoparticle morphologies. *Angew. Chemie - Int. Ed.* **51**, 9078–9082 (2012).
282. Zhou, Y., Huang, Z., Yang, R. & Liu, J. Selection and Screening of DNA Aptamers for Inorganic Nanomaterials. *Chem. - A Eur. J.* **24**, 2525–2532 (2018).
283. Satyavolu, N. S. R., Tan, L. H. & Lu, Y. DNA-Mediated Morphological Control of Pd-Au Bimetallic Nanoparticles. *J. Am. Chem. Soc.* **138**, 16542–16548 (2016).
284. Gugliotti, L. A., Feldheim, D. L. & Eaton, B. E. RNA-mediated control of metal nanoparticle shape. *J. Am. Chem. Soc.* **127**, 17814–17818 (2005).
285. Feldheim, D. L. & Eaton, B. E. Selection of biomolecules capable of mediating the formation of nanocrystals. *ACS Nano* **1**, 154–159 (2007).
286. Berti, L. & Burley, G. A. Nucleic acid and nucleotide-mediated synthesis of inorganic nanoparticles. *Nat. Nanotechnol.* **3**, 81–87 (2008).
287. Bousmail, D., Chidchob, P. & Sleiman, H. F. Cyanine-Mediated DNA Nanofiber Growth with Living Character and Controlled Dimensionality. *J. Am. Chem. Soc.* **140**, 9518–9530 (2018).
288. Zhang, K., Yeung, M. C.-L., Leung, S. Y.-L. & Yam, V. W.-W. Living supramolecular polymerization achieved by collaborative assembly of platinum(II) complexes and block copolymers. *Proc. Natl. Acad. Sci.* **114**, 11844–11849 (2017).
289. Hua, Z. *et al.* Anisotropic polymer nanoparticles with controlled dimensions from the morphological transformation of isotropic seeds. *Nat. Commun.* **10**, 5406 (2019).
290. Glover, D. J., Giger, L., Kim, S. S., Naik, R. R. & Clark, D. S. Geometrical assembly of ultrastable protein templates for nanomaterials. *Nat. Commun.* **7**, 1–9 (2016).
291. Tikhomirov, G., Petersen, P. & Qian, L. Fractal assembly of micrometre-scale DNA origami arrays with arbitrary patterns. *Nature* **552**, 67–71 (2017).
292. Praetorius, F. & Dietz, H. Self-assembly of genetically encoded DNA-protein hybrid



- nanoscale shapes. *Science (80-. )*. **355**, eaam5488 (2017).
293. Nielsen, P. E., Egholm, M., Berg, R. H. & Buchardt, O. L. E. Sequence-Selective Recognition of DNA by Strand Displacement with a Thymine-Substituted Polyamide. *Science (80-. )*. **254**, 1497–1500 (1991).
  294. Kumar, S., Pearce, A., Liu, Y. & Taylor, R. E. Modular self-assembly of gamma-modified peptide nucleic acids in organic solvent mixtures. *Nat. Commun.* **11**, 1–10 (2020).
  295. Lutz, J.-F. F., Lehn, J.-M. M., Meijer, E. W. & Matyjaszewski, K. From precision polymers to complex materials and systems. *Nat. Rev. Mater.* **1**, 16024 (2016).
  296. Appukutti, N., Jones, J. R. & Serpell, C. J. Sequence isomerism in uniform polyphosphoesters programmes self-assembly and folding. *Chem. Commun. (Camb)*. **56**, 5307–5310 (2020).
  297. Douglas, S. M. *et al.* Rapid prototyping of 3D DNA-origami shapes with caDNAno. *Nucleic Acids Res.* **37**, 5001–5006 (2009).
  298. Lutz, J. F., Lehn, J. M., Meijer, E. W. & Matyjaszewski, K. From precision polymers to complex materials and systems. *Nat. Rev. Mater.* **1**, 1–14 (2016).
  299. Edwardson, T. G. W., Carneiro, K. M. M., Serpell, C. J. & Sleiman, H. F. An efficient and modular route to sequence-defined polymers appended to DNA. *Angew. Chemie - Int. Ed.* **53**, 4567–4571 (2014).
  300. Gunay, U. S. *et al.* Chemoselective Synthesis of Uniform Sequence-Coded Polyurethanes and Their Use as Molecular Tags. *Chem* **1**, 114–126 (2016).
  301. Dong, R. *et al.* Sequence-defined multifunctional polyethers via liquid-phase synthesis with molecular sieving. *Nat. Chem.* **11**, 136–145 (2019).
  302. Wenz, N. L. *et al.* Building expanded structures from tetrahedral DNA branching elements, RNA and TMV protein. *Nanoscale* **10**, 6496–6510 (2018).
  303. Wege, C. & Koch, C. From stars to stripes: RNA-directed shaping of plant viral protein templates—structural synthetic virology for smart biohybrid nanostructures. *Wiley Interdiscip.*



*Rev. Nanomedicine Nanobiotechnology* **12**, 1–44 (2020).

304. Mukherjee, S., Pfeifer, C. M., Johnson, J. M., Liu, J. & Zlotnick, A. Redirecting the coat protein of a spherical virus to assemble into tubular nanostructures. *J. Am. Chem. Soc.* **128**, 2538–2539 (2006).
305. Mikkilä, J. *et al.* Virus-encapsulated DNA origami nanostructures for cellular delivery. *Nano Lett.* **14**, 2196–2200 (2014).
306. Ng, B. C., Chan, S. T., Lin, J. & Tolbert, S. H. Using polymer conformation to control architecture in semiconducting polymer/viral capsid assemblies. *ACS Nano* **5**, 7730–7738 (2011).
307. Zeng, C., Rodriguez Lázaro, G., Tsvetkova, I. B., Hagan, M. F. & Dragnea, B. Defects and Chirality in the Nanoparticle-Directed Assembly of Spherocylindrical Shells of Virus Coat Proteins. *ACS Nano* **12**, 5323–5332 (2018).
308. Sinn, S. *et al.* Templated Formation of Luminescent Virus-like Particles by Tailor-Made Pt(II) Amphiphiles. *J. Am. Chem. Soc.* **140**, 2355–2362 (2018).
309. Hernandez-Garcia, A. *et al.* Design and self-assembly of simple coat proteins for artificial viruses. *Nat. Nanotechnol.* **9**, 698–702 (2014).
310. Hernandez-Garcia, A., Cohen Stuart, M. A. & De Vries, R. Templated co-assembly into nanorods of polyanions and artificial virus capsid proteins. *Soft Matter* **14**, 132–139 (2017).
311. Jiang, X. *et al.* Plasmid-templated shape control of condensed DNA-block copolymer nanoparticles. *Adv. Mater.* **25**, 227–232 (2013).
312. Wilks, T. R., Pitto-Barry, A., Kirby, N., Stulz, E. & O'Reilly, R. K. Construction of DNA-polymer hybrids using intercalation interactions. *Chem. Commun.* **50**, 1338–40 (2014).
313. Nguyen, L., Döblinger, M., Liedl, T. & Heuer-Jungemann, A. DNA-Origami-Templated Silica Growth by Sol–Gel Chemistry. *Angew. Chemie - Int. Ed.* **58**, 912–916 (2019).
314. Pang, X., He, Y., Jung, J. & Lin, Z. 1D nanocrystals with precisely controlled dimensions, compositions, and architectures. *Science (80-. ).* **353**, 1268–1272 (2016).



315. Yuan, J. *et al.* Water-soluble organo-silica hybrid nanowires. *Nat. Mater.* **7**, 718–722 (2008).
316. Lucon, J. *et al.* Use of the interior cavity of the P22 capsid for site-specific initiation of atom-transfer radical polymerization with high-density cargo loading. *Nat. Chem.* **4**, 781–788 (2012).
317. Atsumi, H. & Belcher, A. M. DNA Origami and G-quadruplex hybrid complexes induce size control of single-walled carbon nanotubes via biological activation. *ACS Nano* **12**, 7986–7995 (2018).
318. Cai, J. *et al.* Tailored multifunctional micellar brushes via crystallization-driven growth from a surface. *Science (80-. )*. **366**, 1095–1098 (2019).
319. Kinnear, C., Moore, T. L., Rodriguez-Lorenzo, L., Rothen-Rutishauser, B. & Petri-Fink, A. Form Follows Function: Nanoparticle Shape and Its Implications for Nanomedicine. *Chem. Rev.* **117**, 11476–11521 (2017).
320. Toy, R., Peiris, P. M., Ghaghada, K. B. & Karathanasis, E. Shaping cancer nanomedicine: The effect of particle shape on the in vivo journey of nanoparticles. *Nanomedicine* **9**, 121–134 (2014).
321. Li, X. Size and shape effects on receptor-mediated endocytosis of nanoparticles. *J. Appl. Phys.* **111**, 024702 (2012).
322. Chithrani, B. D., Ghazani, A. A. & Chan, W. C. W. Determining the size and shape dependence of gold nanoparticle uptake into mammalian cells. *Nano Lett.* **6**, 662–668 (2006).
323. Hultgren, A., Tanase, M., Chen, C. S. & Reich, D. H. High-yield cell separations using magnetic nanowires. *IEEE Trans. Magn.* **40**, 2988–2990 (2004).
324. Prina-Mello, A., Diao, Z. & Coey, J. M. D. Internalization of ferromagnetic nanowires by different living cells. *J. Nanobiotechnology* **4**, 9 (2006).
325. Wilhelm, C., Gazeau, F. & Bacri, J. C. Rotational magnetic endosome microrheology: Viscoelastic architecture inside living cells. *Phys. Rev. E - Stat. Physics, Plasmas, Fluids, Relat. Interdiscip. Top.* **67**, 12 (2003).



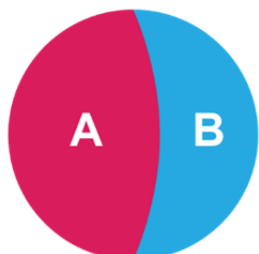
- 326. Hudson, Z. M., Lunn, D. J., Winnik, M. A. & Manners, I. Colour-tunable fluorescent multiblock micelles. *Nat. Commun.* **5**, 1–8 (2014).
- 327. Li, A. *et al.* Synthesis and direct visualization of dumbbell-shaped molecular brushes. *ACS Macro Lett.* **1**, 241–245 (2012).
- 328. Dietz, H., Douglas, S. M. & Shih, W. M. Folding DNA into twisted and curved nanoscale shapes. *Science (80-. )*. **325**, 725–730 (2009).
- 329. Knez, M. *et al.* Biotemplate synthesis of 3-nm nickel and cobalt nanowires. *Nano Lett.* **3**, 1079–1082 (2003).



## Box 1 | Types of Anisotropy

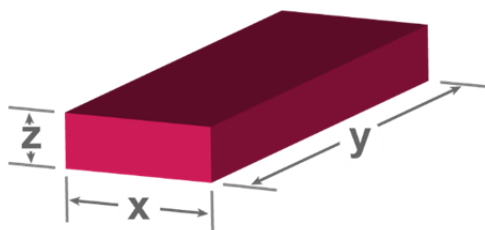
Anisotropy is defined as the display of direction-dependent behaviour. In the context of a nanoparticle, this can manifest itself in three main ways:

### Chemical



The arrangement of chemical groups on the nanoparticle is not homogenous. This could be at the particle surface or throughout the whole structure.

### Shape







The dimensions of the nanoparticle vary between measurement axes. All non-spherical shapes are considered anisotropic. The 'degree' of anisotropy can be measured in different ways, see Box 2.

### Physical Properties



The physical properties of the nanoparticle vary according to the measurement direction. For example, there may be ordered magnetic domains.

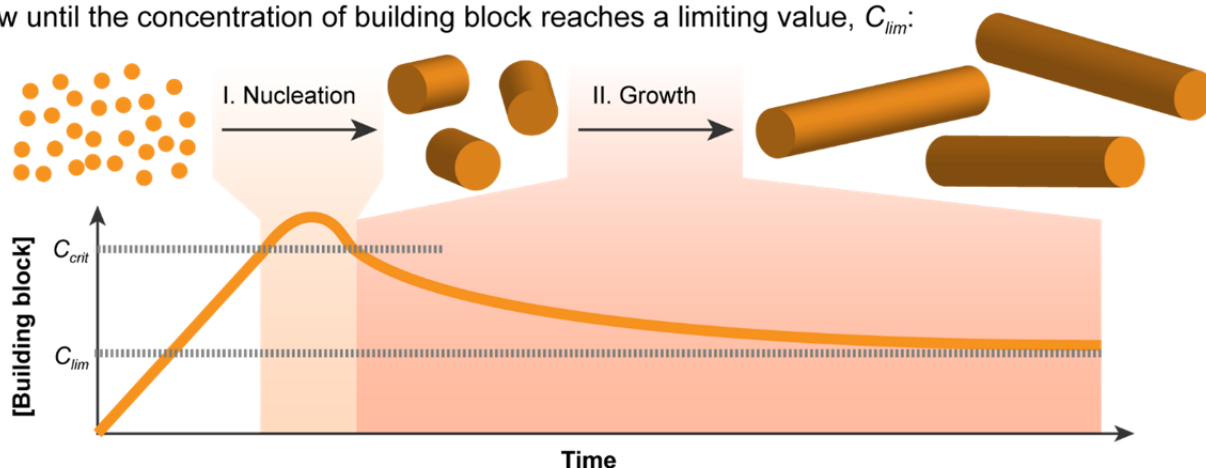
A single nanoparticle may exhibit multiple types of anisotropy, as illustrated by these examples:

Anisotropy				
Shape				
Shape	✓	✗	✓	✓
Chemical	✗	✓	✓	✗
Physical	✗	✗	✗	✓



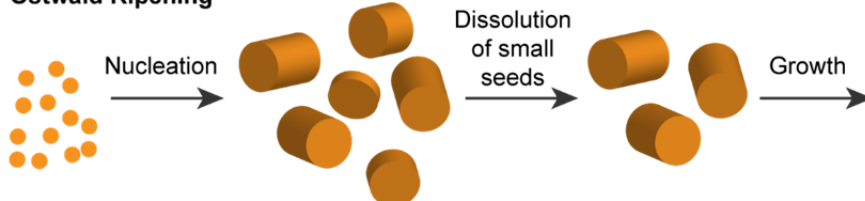
## Box 2 | Crystallisation Mechanisms

Understanding the process of crystallisation is key to achieving control over the resulting products. One of the longest established models is that of LaMer, which separates the nucleation and growth stages. The concentration of a building block increases over time (for example by decomposition of a precursor). At a critical concentration ( $C_{crit}$ ), so called burst nucleation is triggered, leading to the formation of crystal nuclei, or seeds (step I). This causes a drop in the concentration of building block below  $C_{crit}$ , preventing further nucleation. The existing seeds then grow until the concentration of building block reaches a limiting value,  $C_{lim}$ :



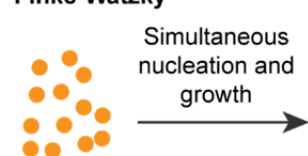
In practice, crystallisation does not always conform to this simple stepwise process. Numerous other models have been developed to account for this, a few of which are outlined below.

### Ostwald Ripening



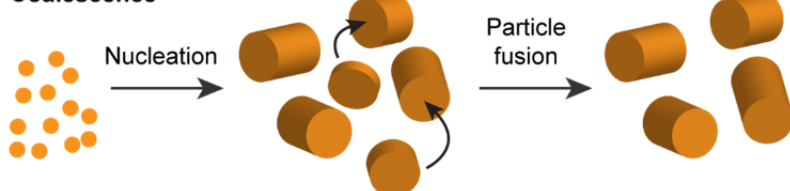
During nucleation, different sized seeds are formed, with stability dependent on their size. Small seeds redissolve, allowing larger seeds to grow at their expense. The inverse of this process (in which large seeds dissolve and small seeds grow) is known as **digestive ripening**.

### Finke-Watzky



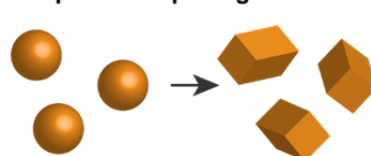
Slow, continuous nucleation is accompanied by autocatalytic surface growth. There is no temporal separation of nucleation and growth.

### Coalescence



Following nucleation, seed particles grow by fusion with one another. Where crystallographic planes are not aligned during this process it is known as **coalescence**; when they are aligned it is known as **oriented attachment**.

### Intraparticle Ripening



A change in the shape of a particle over time. This arises when the only instability in the system is the difference in surface energy between different crystal facets.



**Figure 1. Controlled crystallisation of anisotropic nanoparticles.** Comparison of the two methods for the synthesis of anisotropic nanoparticles by controlled crystallisation. In solvothermal synthesis (route 1), molecular building blocks are mixed in solution and exposed to a set of reaction conditions (including temperature, pH, salts and ligands) for a period of time. To obtain the desired shape and aspect ratio, a single set of reaction conditions must control all stages of crystal growth. Seeded growth (route 2) separates crystal seed formation (step a) and growth (step b). It is therefore possible to optimize the conditions of each step separately, so that tuning of nanoparticle aspect ratio can be achieved by varying the length of the growth step.

**Figure 2. Seeded growth of well-defined anisotropic nanostructures by crystallisation-driven self-assembly (CDSA).** a) Schematic illustration of a typical CDSA seeded growth process. A diblock copolymer containing solvophilic and semi-crystalline blocks is driven to self-assemble into anisotropic nanoparticles by polymer crystallisation (step 1). These size-disperse particles are fragmented, typically by heat or ultrasonication, to generate a population of uniform seed nanoparticles (step 2). Addition of a second polymer free in solution induces anisotropic growth and facilitates the construction of segmented nanostructures with well-defined dimensions. b) Tuning the ratios between the polymer blocks enables control over morphology.<sup>66</sup> c) Selective degradation of one polymer allows access to complex topologies.<sup>262</sup> d) Multiple sequential growth steps with different polymers give rise to patchy, multifunctional nanoparticles.<sup>326</sup> Part b is adapted with permission from ref 54. Part c is adapted with permissions from ref 61. Part d is adapted with permissions from ref 62.

**Figure 3. Programmed assembly for the synthesis of anisotropic nanoparticles.** a) Schematic of the concept of programmed assembly: a macromolecule or macromolecules undergo controlled molecular folding in solution driven by multiple weak interactions. b) Different examples of programmed assembly arranged in order of the complexity of the molecular interactions that drive folding. Single chain nanoparticles (SCNPs,



left) are made from polymers that fold on themselves. In this example, sequential polymerisation of monomers with different lengths leads to a dumbbell-shaped bottlebrush SCNP. An atomic force microscopy image of the dumbbell is shown above an illustration of the designed polymer structure.<sup>327</sup> DNA nanotechnology (middle) makes use of the highly predictable pairing between nucleotides to achieve the programmed assembly of a wide array of nanoscale shapes. Here, curvature has been introduced to form gear-shaped structures. a negative stain TEM image is shown above the in silico design.<sup>328</sup> Protein engineering (right) seeks to achieve the same goal with polypeptides, which are more functionally diverse than nucleic acids but also much harder to rationally design. In this example, barrel-shaped assemblies have been designed with exquisite control over pore diameter. Top and side views of the X-ray crystal structures of two different barrel designs are shown.<sup>101</sup> Part b (left) is adapted with permissions from Ref. 84. Part b (centre) is adapted with permissions from ref 85. Part b (right) is adapted with permissions from ref 86..

**Figure 4. Approaches to the templated assembly of anisotropic nanoparticles.** a) Coating. A template nanoparticle is coated in a second material. This approach is conceptually simple but does not permit re-use of the template. In DNA origami silicification (DOS)<sup>113</sup> (bottom) silica nanostructures are grown from DNA origami templates.; b) Casting. A hollow nanoparticle is used as a mould to constrain growth of a second material. The template can be removed and possibly reused. The tobacco mosaic virus has been used to direct the controlled growth of Ni and Co nanowires within their interior compartment. A TEM image of a Co nanowire within the virus is shown.<sup>329</sup> c) Breadboard. A nanoparticle is used as a platform to pattern building blocks, which are then fused. Template removal and re-use is simplified. DNA nanotechnology can direct assembly of Au nanostructures using a 2D DNA origami sheet as template. Here, a box-shaped octamer is shown by TEM.<sup>132</sup> Part a is adapted with permission from Ref. 103. Part b is adapted with permission from ref. 111. Part c is adapted with permission from ref.112



**Figure 5. Exploiting precise dimensional control to enable advanced therapeutic applications.**

The aspect ratio of a gold nanorod is tuned so that its absorption maximum coincides with the wavelength of a NIR laser. Coating of the nanorods with antibodies enables their targeting to malignant cells. Irradiation with a NIR laser enables specific destruction of diseased cells while leaving healthy cells intact and leads to increased tissue penetration depth (adapted from reference <sup>145</sup>).

**Figure 6. Control of optical properties.** Control over nanoparticle dimensions allows optical properties to be tuned for specific applications. a) Altering the anisotropic shape of a Au nanoparticle results in changes in its absorption spectrum, allowing the absorption maximum to be selected to fit within a desired optical window. b) The anisotropic shape of metal nanoparticles can be tuned to optimise surface-enhanced Raman scattering (SERS) enhancement. c) The photoluminescence of anisotropic perovskite nanoparticles can be modulated by controlling the thickness and aspect ratio. (a, b adapted from reference <sup>21</sup>, c adapted from reference <sup>154</sup>)

**Figure 7. Advanced electronic materials realised by controlled anisotropic nanoparticle growth.** a) segmented semi-conducting nanofibers through multistep CDSA with an A-B-A structure for separate donor and acceptor domains, b) the properties can be optimised by tuning the domain sizes of the conjugated nanoparticle core and energy-accepting corona, to realise exceptional exciton transport properties (adapted from reference <sup>167</sup>).

**Figure 8. Catalytic and magnetic properties of anisotropic nanoparticles.** a) Nanoparticle shape influences catalytic properties through selective presentation of active crystal facets<sup>170</sup>. b) Anisotropic and magnet-



ic particles allow field-tuning of reflection spectra with respect to the direction of light, for applications as photonic crystals<sup>190</sup>. Part a is adapted from reference <sup>170</sup>. Part b adapted from reference <sup>190</sup>.

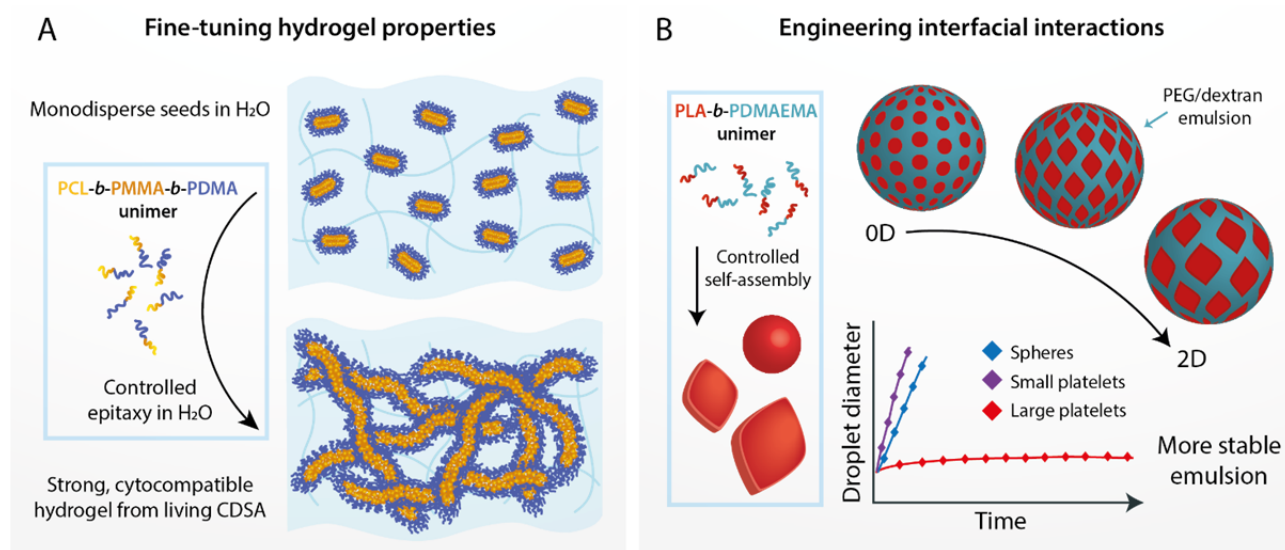


**Figure 9. Modulating fluid properties using anisotropic nanoparticles.** a) Well-defined 1D anisotropic nanoparticles grown using crystallisation-driven self-assembly (CDSA) can be used to form strong, biocompatible hydrogels. Changes in aspect ratio and shape allow the properties to be tuned further<sup>71</sup>. b) 2D anisotropic nanoparticles can act as stabilisers for Pickering emulsions, with large platelets giving enhanced performance compared to small platelets and spheres<sup>242</sup>. Part a is adapted from reference 59. Part b is adapted from reference 213.

**Figure 10. The effects of particle anisotropy on biological processing.** a) Nanoparticle shape not only influences cell uptake efficiency, but also cellular signalling. In this example the size of 2D nanoplates was related to the level of expression of pro-inflammatory cytokines<sup>269</sup>) b) The effects of particle anisotropy also manifest themselves at the level of a whole organism. In this example anisotropic cylinders demonstrate prolonged blood circulation and increased therapeutic effect (evidenced by decreased leukocytes concentration) compared with isotropic control particles<sup>255</sup> c) The effects of particle anisotropy can be exploited to direct tissue accumulation. In this example particle size could



directly positively influence tumour uptake with reduced sequestration into organs such as liver and spleen<sup>272</sup>. Part a is adapted from ref. 245. Part b is adapted from ref. 240. Part c is adapted from ref. 246.

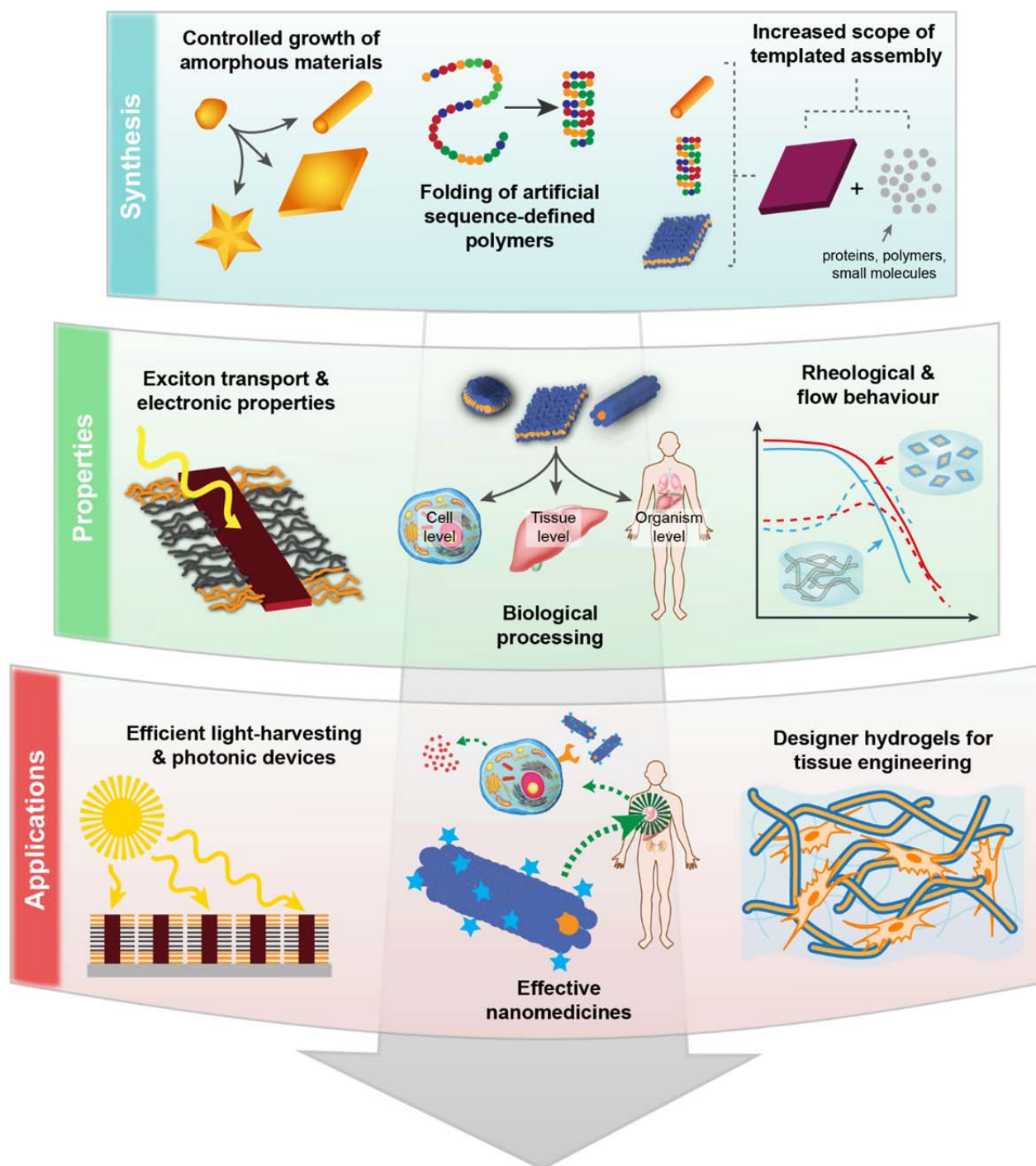


**Figure 11. A roadmap for future research on the synthesis, properties and applications of precision anisotropic nanoparticles.** Development of new synthetic techniques will underpin future progress by enabling a



greater diversity of materials to be used as nanoparticle building blocks. This increased diversity will enable the study of fundamental properties by allowing structure–function relationships to be determined for the first time in a wide range of areas. Finally, this greatly improved fundamental understanding will enable rational design of anisotropic nanoparticles for particular applications.

Table of Contents graphic